Molecular Therapy
Methods & Clinical Development
Original Article

FastAd: A versatile toolkit for rapid generation of single adenoviruses or diverse adenoviral vector libraries

Shao-Chia Lu,[1] Yi-Yuan Lee,[2] Felix G.M. Andres,[1] Daniel A. Moyer,[3,4] and Michael A. Barry[1,4,5]

[1]Division of Infectious Diseases, Department of Medicine, Mayo Clinic, Rochester, MN 55905, USA; [2]Department of Computational Biology, Cornell University, Ithaca, NY 14850, USA; [3]Immunology Track, Mayo Clinic Graduate School of Biomedical Sciences, Rochester, MN 55905, USA; [4]Department of Immunology, Mayo Clinic, Rochester, MN 55905, USA; [5]Department of Molecular Medicine, Mayo Clinic, Rochester, MN 55905, USA

Adenoviruses (Ads) are potent gene delivery vectors for *in vitro* and *in vivo* applications. However, current methods for their construction are time-consuming and inefficient, limiting their rapid production and utility in generating complex genetic libraries. Here, we introduce FastAd, a rapid and easy-to-use technology for inserting recombinant "donor" DNA directly into infectious "receiver" Ads in mammalian cells by the concerted action of two efficient recombinases: Cre and Bxb1. Subsequently, the resulting mixed recombinant Ad population is subjected to negative selections by flippase recombinase to remove viruses that missed the initial recombination. With this approach, recombinant Ad production time is reduced from 2 months to 10 days or less. FastAd can be applied for inserting complex genetic DNA libraries into Ad genomes, as demonstrated by the generation of barcode libraries with over 3 million unique clones from a T25 flask-scale transfection of 3 million cells. Furthermore, we leveraged FastAd to construct an Ad library containing a comprehensive genome-wide CRISPR-Cas9 guide RNA library and demonstrated its effectiveness in uncovering novel virus-host interactions. In summary, FastAd enables the rapid generation of single Ad vectors or complex genetic libraries, facilitating not only novel applications of Ad vectors but also research in foundamental virology.

INTRODUCTION

Adenoviruses (Ads) are widely used viral vectors in basic research and translational applications, including genetic vaccines, gene therapies, and oncolytic viruses.[1–5] Ads offer several useful features, including: (1) a large DNA coding capacity (up to 36 kilobase pairs [kbp]), (2) over 100 genetically distinct serotypes/genotypes for varied cellular tropisms, (3) stable virions suitable for lyophilization and long-term storage at ambient temperatures, and (4) scalable good manufacturing practice (GMP) production, as demonstrated by the production of over 3 billion Ad vaccines during the COVID-19 pandemic.[1,6]

Despite these advantages, constructing recombinant Ad vectors is slow and inefficient. Historically, Ad genome modifications have been performed directly on viral DNA (vDNA) or on recombinant plasmids/bacmids by three methods: (1) direct *in vitro* modification using restriction enzymes and ligases,[7,8] (2) homologous recombination in mammalian cells,[9–12] and (3) homologous recombination in bacteria.[13–16] Bacterial homologous recombination is currently the preferred choice due to its higher efficiency and reproducibility, bypassing laborious plaque purification processes typically required by other methods.[13–15] However, this method also has a major drawback: inherently low efficiency in generating infectious viruses from bacteria-derived DNA.

For example, 1 μg of a 36 kbp recombinant Ad DNA contains approximately 3×10^{10} viral genomes, but only about 50 infectious viral clones are rescued from this amount of DNA.[17] This low efficiency, with just 1 in 6×10^{8} recombinant Ad DNAs becoming infectious, is primarily due to the absence of adenoviral terminal proteins (TPs) on bacteria-derived Ad DNA, which are essential for nuclear localization and initiating viral replication.[18–20] TP-deficient Ad DNA is 100 to 1,000 times less efficient in producing infectious virus compared with naturally TP-capped Ad DNA.[21,22] As a result, virus rescue is slow, requiring serial amplification in larger cultures and extending the process to up to 2 months from recombinant DNA to large-scale Ad production.[23,24] This inefficiency is especially problematic during healthcare emergencies, such as pandemics, when rapid vaccine production or adaptation to evolving pathogens is crucial.[25]

Moreover, the inefficiency of converting bacteria-derived recombinant DNA to infectious virus significantly limits the generation of diverse Ad libraries, which are essential for selecting functional transgenes or capsid variants.[26,27] To address the challenge, researchers have explored alternative approaches, including ligating TPs to plasmid-based cDNA libraries[28] or using the Cre/*loxP* recombinase system to produce recombinant Ads.[26,29–31] While these systems offer improvements over the classical workflow, there remains a need for a

Received 11 July 2024; accepted 15 October 2024;
https://doi.org/10.1016/j.omtm.2024.101356.

Correspondence: Michael A. Barry, Division of Infectious Diseases, Department of Medicine, Mayo Clinic, Rochester, MN 55905, USA.
E-mail: mab@mayo.edu

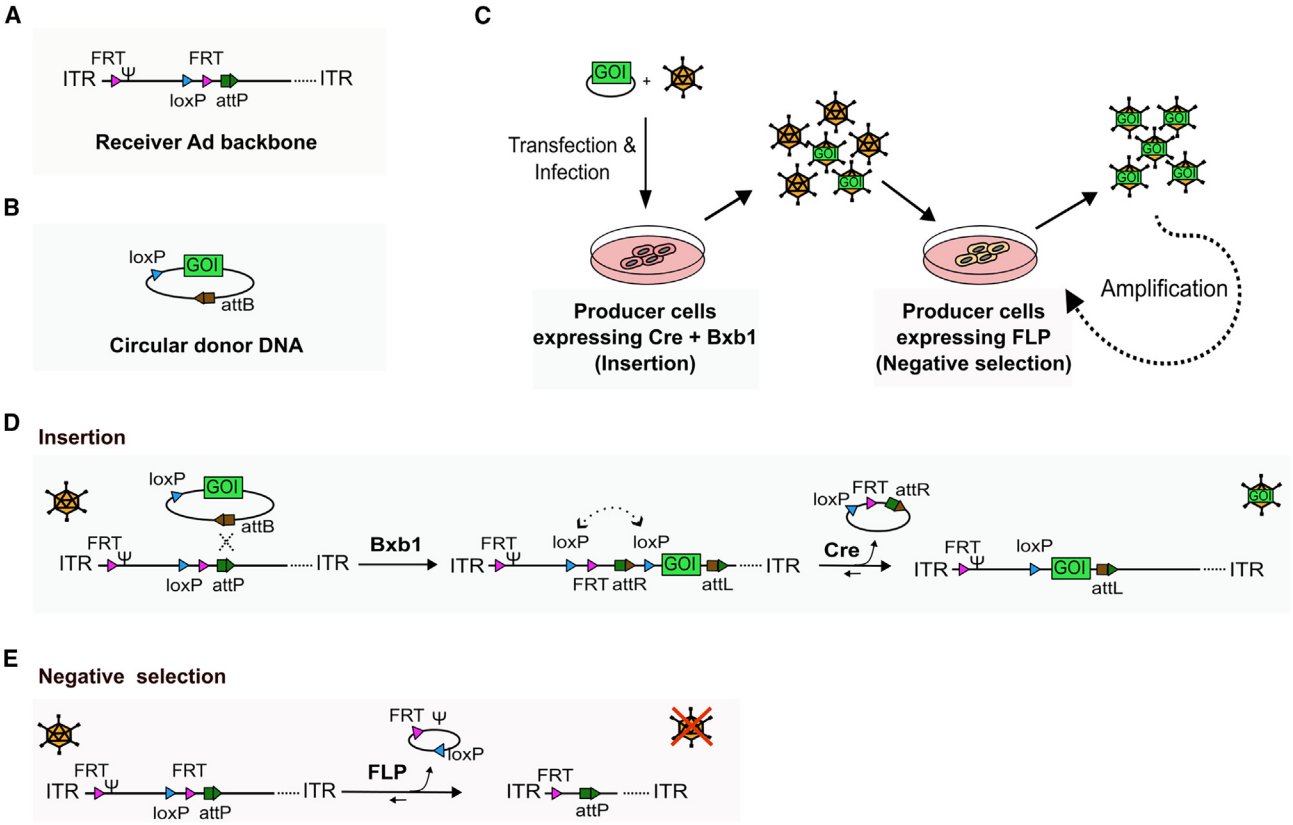

Figure 1. The design logic of the FastAd system

(A) The Ψ and basic recombinase recognition sites on receiver Ad backbone. Ψ, adenoviral packaging signal; ITR inverted terminal repeat; attP, phage attachment site of Bxb1. (B) The basic recombinase recognition sites on circular donor DNA. attB, bacterial attachment site of Bxb1. (C) The components and general workflow for recombinant Ad production by FastAd. Transfected DNA fragments are inserted into receiver Ads by Cre and Bxb1 in the first producer cell line, followed by a negative selection within the second producer cell line expressing FLP. (D) Insertion of donor DNA mediated by Bxb1 and Cre. attL/attR, attachment site left/right. (E) Negative selection: excision of Ψ by FLP.

more convenient, efficient, and versatile tool that can better support diverse research goals.

To expedite Ad production and generate large-scale genetic Ad libraries, we present FastAd. FastAd is an easy-to-use Ad vector construction method with three components: (1) an infectious receiver Ad vector with naturally TP-capped genomes, (2) recombinant donor DNA from synthesis, PCR, or plasmids, and (3) two producer cell lines expressing Cre/Bxb1 or flippase (FLP) recombinase. By utilizing these recombinases, FastAd enables precise insertion of recombinant DNA into Ad genomes and removes the majority of non-integrated receiver Ads through negative selection. We verified the FastAd's efficiency in generating individual Ads and complex Ad libraries in this study.

RESULTS

FastAd strategy

To circumvent the laborious and time-consuming process of cloning/rescuing adenoviral vectors, we designed FastAd. This method facilitates the direct insertion of recombinant DNA into the genomes of receiver Ads within infected mammalian cells using Cre and Bxb1 recombinases. While Cre mediates recombination between *loxP* sites, Bxb1, a large serine recombinase, recognizes minimal 48-bp attP (attachment phage) and 38-bp attB (attachment bacterial) sites. Bxb1 mediates irreversible and unidirectional integration of donor DNA,[32,33] thus promoting the formation of integrated Ads, which contrasts with the reversible nature of the Cre/*loxP* system. In addition, FLP-FRT recombination, which mediates recombination between two FRT sites and was shown to efficiently delete Ad packaging signal (Ψ) in the helper-dependent adenoviral vectors,[34] is implemented for negative selection in FastAd.

Receiver Ads were designed to contain a landing region containing a *loxP* site, an FRT site, and an attP site for recombination of incoming donor DNA (Figure 1A). To negatively select against Ads that escape the insertion of incoming donor DNA, the other FRT site was placed at the 5′ end of the Ψ. Circular DNA donor shuttles contain a gene of interest (GOI) flanked by one *loxP* site and one attB site (Figure 1B). Producer cells were generated to express Cre and Bxb1 or FLP to act upon these cassettes (Figure 1C).

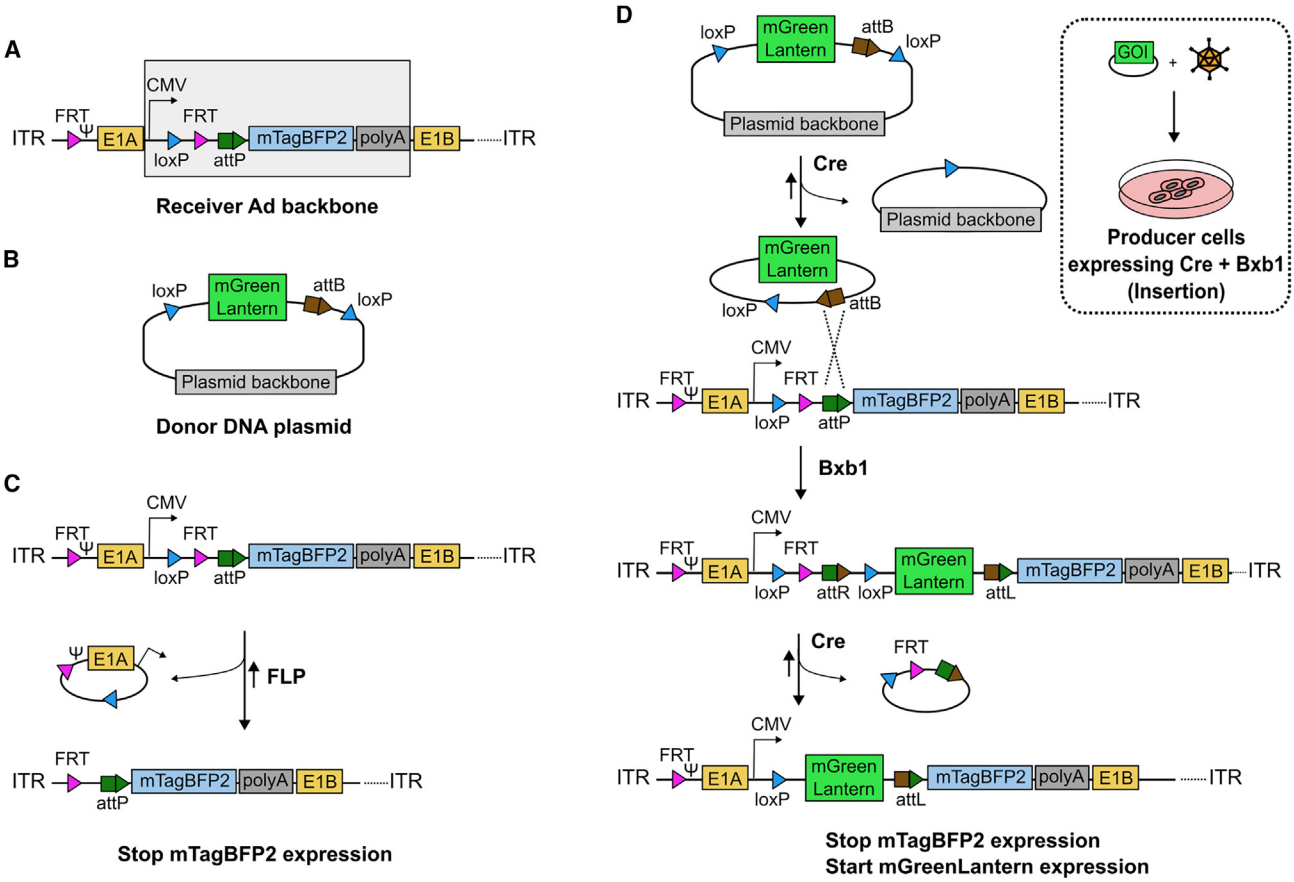

Figure 2. Vector backbones for testing the efficiency of the FastAd system by fluorescent protein reporters

(A) Receiver RC-Ad6-mTagBFP2 backbone with the FastAd cassette containing a CMV promoter and a mTagBFP2 reporter between the *E1A* and *E1B* genes. CMV, human cytomegalovirus immediate-early promoter; poly(A), polyadenylation signal. (B) Donor DNA plasmid with a *loxP*-mGreenLantern-attB-*loxP* cassette. (C) Negative selection mechanism by FLP-mediated excision of Ψ. The efficiency of negative selection can be evaluated by the loss of mTagBFP2 expression in infected cells. (D) Insertion of mGreenLantern gene by Bxb1 and Cre. The final form of integrated Ads is not susceptible to negative selection.

FastAd recombination is initiated by transfection of donor DNA followed by infection with the receiver Ads in the Cre- and Bxb1-expressing cells (Figure 1C). When the Bxb1-mediated DNA integration events take place, integrated Ads enter an intermediate state wherein the second FRT site (toward the 3′ end of the Ad genomes) is flanked by two *loxP* sites. The recombinase activity of Cre favors deleting this second FRT site on the genome (Figure 1D), thus preventing the Ψ on integrated Ads to be deleted in FLP-expressing cells. In contrast, if no GOI is inserted, FLP will delete the Ψ, generating a viral genome that cannot be packaged or propagated (Figure 1E). Viruses are then serially amplified in the FLP-expressing cell line to eliminate all non-integrated receiver viruses containing two FRT sites (Figure 1C).

Testing and benchmarking the efficiency of FastAd

As a proof-of-concept, we constructed a replication-competent receiver Ad backbone (RC-Ad6-mTagBFP2) with an FRT site to the left of Ψ and, at the same time, incorporated a FastAd integration cassette between the Ad *E1A* and *E1B* genes. This cassette consists of a human cytomegalovirus (CMV) immediate-early promoter, a *loxP* site, an FRT site, an attP site, a blue fluorescent protein reporter (*mTagBFP2*) gene, and a bovine growth hormone (bGH) polyadenylation signal (Figure 2A). For donor DNA, a plasmid was constructed containing a green fluorescent reporter (*mGreenLantern*) gene and an attB site, both flanked by two *loxP* sites (Figure 2B).

When the receiver Ads enter FLP-expressing cells, Ψ, *E1A* gene, and CMV promoter responsible for driving *mTagBFP2* expression, will be deleted (Figure 2C). Therefore, loss of mTagBFP2 expression marks the elimination of Ψ from Ads that escape the initial integration by Cre/Bxb1. On the other hand, when we provide mGreenLantern donor DNA plasmids into the Cre- and Bxb1-expressing producer cell line, the backbone sequences of donor DNA plasmid (antibiotic resistance gene and origin of replication) that are flanked by two *loxP* sites will be removed by Cre. This process yields a ready-to-integrate, circular *loxP*-mGreenLantern-attB donor DNA fragment

(Figure 2D). When this circular DNA donor fragment is inserted into the receiver Ad backbones by Bxb1, this integration generates an intermediate Ad with the second FRT site flanked by two *loxP* sites. The second FRT site is subsequently eliminated by Cre, resulting in the desired mGreenLantern-expressing recombinant Ad that resists FLP-mediated negative selection (Figure 2D).

Alternatively, at lower efficiency, the donor DNA can also undergo integration by Cre, followed by Bxb1 cleaving the FRT sites with the attP/attB pair (Figures S1A and S1B). Because of the existence of this alternative integration pathway (Figure S1B), we can evaluate not only the efficiency of FastAd by assessing the intensity of mTagBFP2 and mGreenLantern fluorescence signals in infected cells, but also compare its efficiency to the Cre/*loxP* integration system that is only mediated by Cre.[31]

To assess the efficiency of negative selection, 293 and 293-FLP cells were infected with 1,000 viral particles (vp) per cell of the receiver virus, RC-Ad6-mTagBFP2. After 48 h, it was observed that 99.6% of the 293 cells were positive for mTagBFP2, while only 1.34% of 293-FLP were mTagBFP2 positive (Figure 3A), demonstrating the efficiency of negative selection for eliminating non-integrated receiver Ads.

To test the efficiency of donor DNA insertion, 293, 293-Cre, and 293-Cre+Bxb1 cell lines were transfected with or without mGreenLantern donor plasmids. After 16 h, these cells were infected with receiver RC-Ad6-mTagBFP2 or left untreated (Figure 3B). Flow cytometry analysis at 48 h after infection demonstrated a substantial increase in mGreenLantern-positive cells to 66.6% in 293-Cre+Bxb1 cells (Figure 3C). In contrast, 293-Cre had a less substantial increase in mGreenLantern positivity (35.24%). The negative control 293 cells displayed only minimal mGreenLantern fluorescence, representing the background signal (7.93% total) (Figure 3C). Significantly, a distinct population exclusively expressing mGreenLantern (30.3%) was observed in the 293-Cre+Bxb1 producer cells, a percentage markedly higher than that observed in the 293-Cre (2.54%) and 293 cells (0.19%) (Figure 3C). This observation indicates that the mGreenLantern DNA fragments have successfully been integrated into a large portion of receiver Ads even before the transcription of mTagBFP2 from the original backbone.

In the negative selection scenario, Cre alone lacks the capability to remove the second FRT site from the receiver Ad backbone (Figure S1B). When the mixed Ad population produced from 293-Cre cells (Cre/*loxP* system) was used to infect 293-FLP cells, there was a notable decrease in both mTagBFP2 and mGreenLantern's expression level when compared with the results in 293 cells (Figure 3D).

When using the Ad population derived from 293-Cre+Bxb1 cells (FastAd) to infect 293 cells, most cells are both mTagBFP2 and mGreenLantern positive (Figure 3E). In contrast, when infecting 293-FLP cells, minimal mTagBFP2 signal from the non-integrated receiver virus was observed, and almost all cells exclusively expressed mGreenLantern (Figure 3E). These findings suggest that genes of interest are efficiently knocked into the receiver virus in 293-Cre+Bxb1 cells, while elimination of non-integrated receiver viruses is achieved in 293-FLP cells.

Flow cytometry assesses the efficiency of FastAd by reporter gene expression, but it does not provide information at the DNA level. To address this, total genomic DNA (gDNA) from the transfected/infected cells were analyzed by quantitative PCR (qPCR) to detect integrated mGreenLantern DNA fragments. To distinguish the amplified mGreenLantern DNA fragments in Ad genomes by viral replication from those in transfected donor plasmids, we designed the qPCR amplicon to comprise two DpnI restriction endonuclease sites. When this DNA is treated with DpnI, methylated DNA derived from bacteria is digested,[35] while unmethylated viral and mammalian DNA stays intact (Figure 3F). By this approach, a 50-fold increase in the number of mGreenLantern copies within Ad genomes was observed in 293-Cre+Bxb1 cells when compared with 293-Cre cells (Figure 3G). Despite the moderate mGreenLantern expression observed in flow cytometry analysis from 293-Cre cells (Figure 3C), only minimal amounts of mGreenLantern DNA were amplified from these cells (Figure 3G). This implies that these fragments were primarily shuffling between Ad genomes without undergoing viral replication in 293-Cre cells. Also, FLP-mediated negative selection increased the ratio of mGreenLantern DNA copies to Ad-hexon DNA copies (Figure 3H), demonstrating the efficient removal of non-integrated Ads by negative selection with FLP.

Evaluating the purity and the quality of recombinant Ads produced by FastAd

To evaluate the purity of the final recombinant Ad preps from FastAd, the viruses from each T25 flask transfection were amplified through five passages in either 293 cells or 293-FLP cells until reaching the scale of a 10-layer CellSTACK culture chamber (6,360 cm^2) over the course of 18 days (Figure 4A). These viruses were purified on CsCl gradients. A549 cells were infected at varying multiplicity of infections (MOIs) (50, 1,000, and 10,000 vp/cell) of the purified Ads and flow cytometry analysis was performed to detect mTagBFP2 and mGreenLantern expression. Consistent with earlier findings, Ads grown in 293-Cre+Bxb1 cells had the highest mGreenLantern reporter activity when compared with other cells (Figure 4B). Importantly, 99.5% of cells infected with 10,000 vp/cell of purified Ads from the 293-Cre+Bxb1 plus negative selection group ($Cre^+Bxb1^+FLP^+$) were almost exclusively positive for mGreenLantern and negative for mTagBFP2. The level of mGreenLantern expression was similar to that expressed by a positive control Ad vector, where an identical mGreenLantern integration was achieved by traditional recombination method in bacteria (Figure 4B).

To obtain more quantitative information on mGreenLantern integration efficiency and compare the distribution of integrated and non-integrated Ads in the purified virus stocks, purified vDNA was analyzed by Sanger sequencing (Figure 4C). Ads from $Cre^-Bxb1^-FLP^-$ and $Cre^+Bxb1^-FLP^-$ groups displayed sequencing peaks identical to the reference non-integrated receiver Ad, indicating the integrated

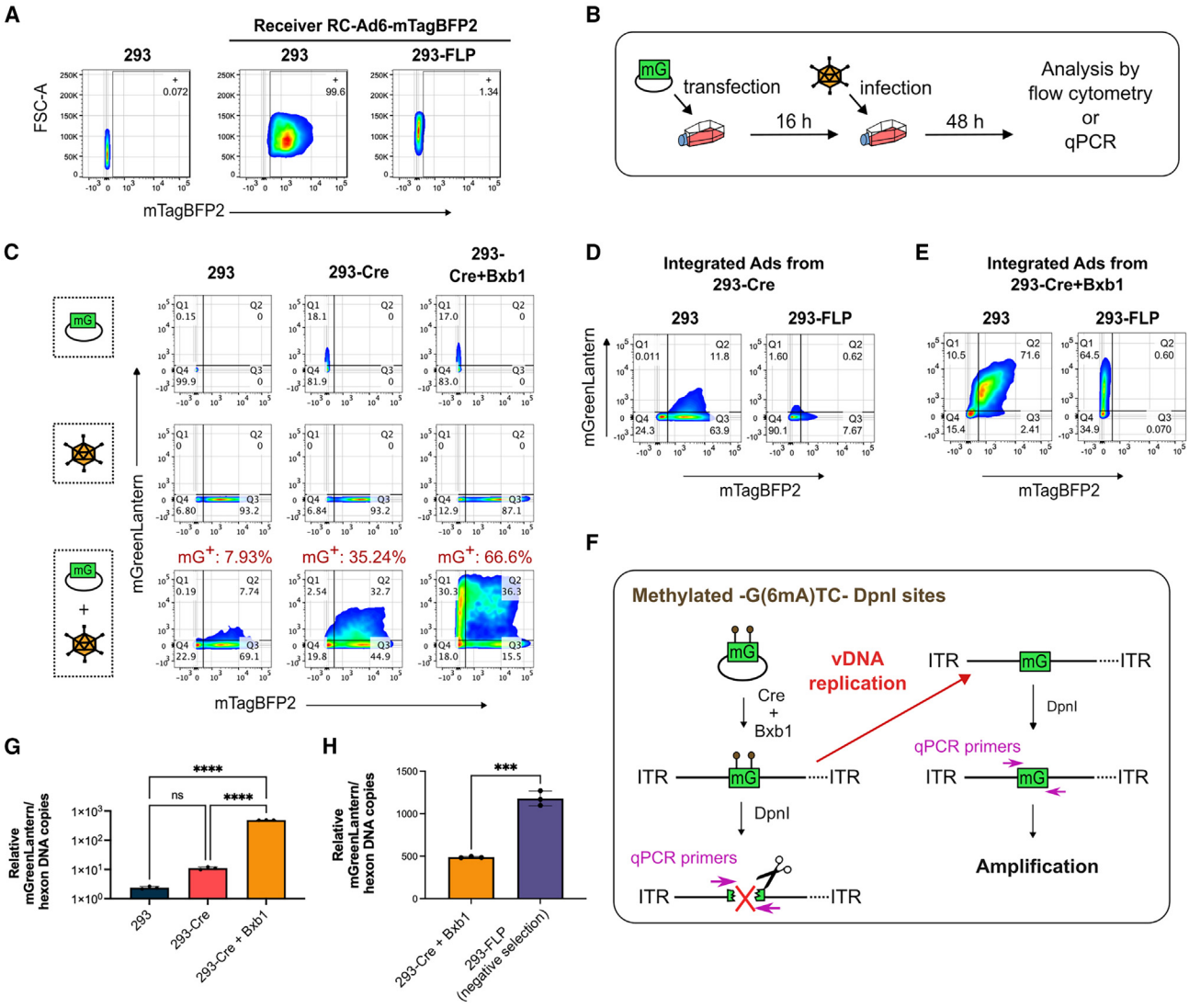

Figure 3. Evaluation of FastAd efficiency

(A) 293-FLP cells were established to remove Ψ from non-integrated Ads. Loss of mTagBFP2-fluorescence in receiver virus-infected 293-FLP cells is indicative for its efficiency. (B) Timeline for the transfection of donor DNA plasmids and infection of FastAd producer cells with receiver Ads. (C) The two-fluorescent protein-based reporter system for evaluating the incorporation efficiency of FastAd and direct comparison with the Cre/*loxP* system. (D) 293 or 293-FLP cells infected with Ads integrated in 293-Cre cells (Cre/*loxP* system). (E) 293 or 293-FLP cells infected with Ads integrated in 293-Cre-Bxb1 cells (FastAd). (F) The qPCR primer set was designed to amplify an amplicon containing two DpnI sites within the mGreenLantern gene. (G) Relative mGreenLantern copies from DpnI-treated total gDNA between 293, 293-Cre, and 293-Cre+Bxb1 cells as quantified by qPCR. The relative amount of mGreenLantern was normalized by Ad-hexon copies as an internal control. Statistics of relative mGreenLantern copies were performed by one-way ANOVA and Tukey's multiple comparisons test (****$p \leq 0.0001$; ns, $p > 0.05$). (H) Relative mGreenLantern copies from DpnI-treated total gDNA samples of 293-Cre+Bxb1 and the sample after negative selection, normalized by Ad-hexon copies in the qPCR assay. Statistics of relative mGreenLantern copies were performed by unpaired t test. (***$p \leq 0.0002$).

population is very low and below the detection limit of Sanger sequencing. In contrast, 5%–14% of Ads from the Cre$^+$Bxb1$^+$FLP$^-$ group contained *mGreenLantern* sequence (Figure 4D), as determineted by the decomposition of the Sanger sequencing result using BEAT software.[36] Significantly, the sequencing results showed the Ad population grown in the Cre$^+$Bxb1$^+$FLP$^+$ group have a completely identical sequence to the positive reference Ads (Figure 4C), highlighting the performance of the negative selection system in removing non-integrated Ads.

qPCR of vDNA confirmed that the integration efficiency in the Cre$^+$Bxb1$^+$FLP$^-$ group (FastAd-integration step only) was 100-fold higher than in vDNA from the Cre$^+$Bxb1$^-$FLP$^-$ group (Cre/*loxP* integration) (Figure 4E). With negative selection in the Cre$^+$Bxb1$^+$FLP$^+$

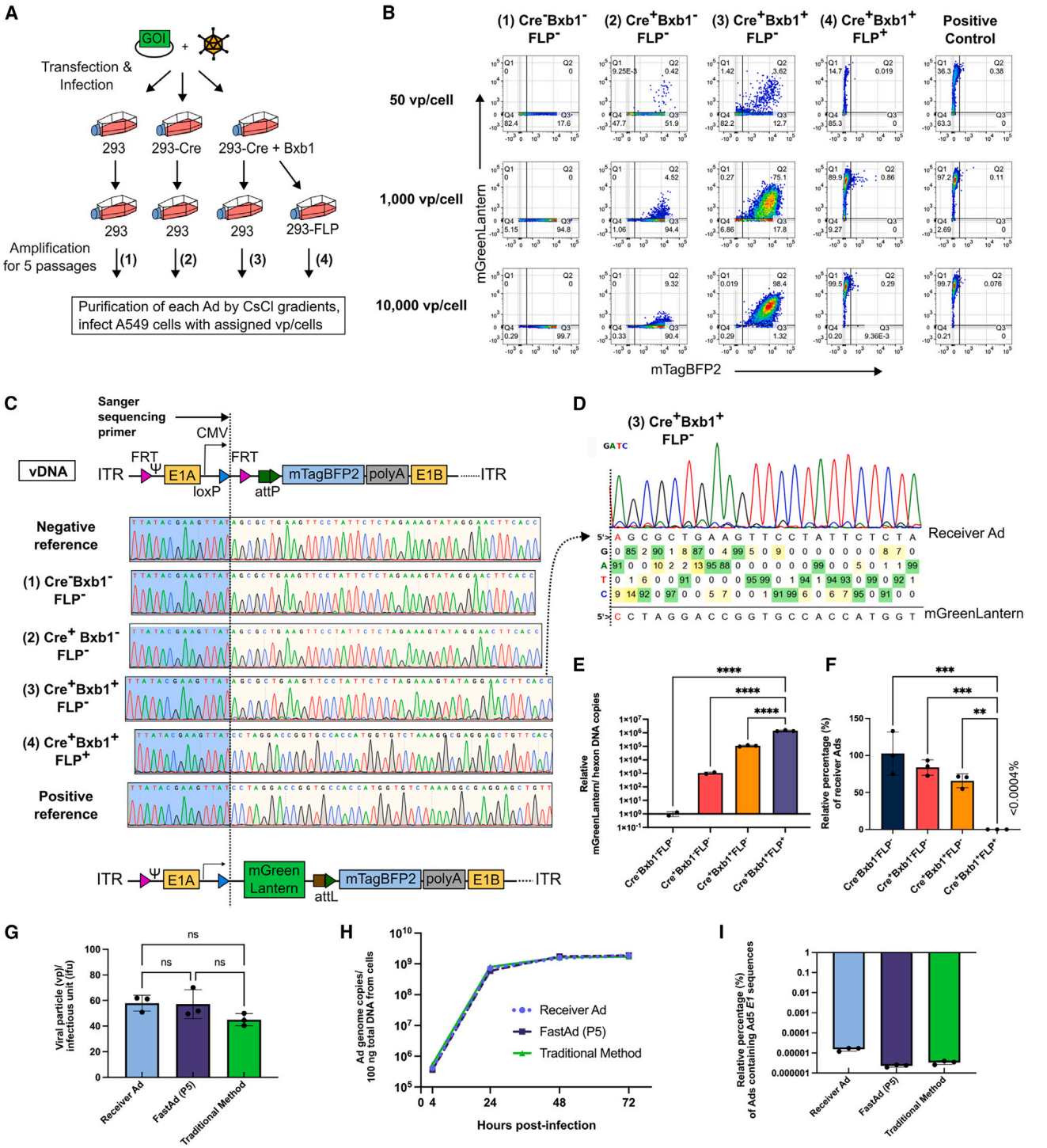

Figure 4. Evaluation of the purity/infectivity/DNA replication of Ads generated by FastAd

(A) Scheme of virus preparation for purity assessment experiments. (B) Purified Ads and the positive control Ad were used to infect A549 cells at MOIs of 50, 1,000 and 10,000 vp/cell to compare the efficiency of FastAd and degree of contamination from the original receiver Ads. (C) The purified vDNA from each group was analyzed by Sanger sequencing with a primer annealing to the CMV promoter. The sequencing peak views were visualized with SnapGene Software. (D) Base calling ratio from the sequencing results of purified Ad DNA from the $Cre^{+}Bxb1^{+}FLP^{-}$ group was analyzed by the BEAT software to evaluate integration efficiency. (E) Relative mGreenLantern copies within purified vDNA, normalized to Ad-hexon copies. Statistics of relative mGreenLantern copies/hexon copies were performed by one-way ANOVA and Tukey's

(legend continued on next page)

group, the integration efficiency was 10-fold higher than in vDNA from $Cre^{+}Bxb1^{+}FLP^{-}$ group and 1,000-fold higher than in vDNA from the $Cre^{+}Bxb1^{-}FLP^{-}$ group (Figure 4E). The prevalence of receiver Ad-specific sequences (*loxP*-FRT-attP cassette) after the negative selection was also confirmed to be extremely low (<0.0004%) in the $Cre^{+}Bxb1^{+}FLP^{+}$ group (Figure 4F), indicating that the FastAd system can yield nearly pure recombinant virus after five negative selection passages.

To assess if the Ads produced from FastAd have similar properties to the Ads made by the traditional recombination method in bacteria, we titered the infectious units (ifu) and determined the vp to ifu ratio of each Ad. By analyzing the receiver Ad (RC-Ad6-mTagBFP2), the mGreenLantern integrated Ad (by FastAd) and the mGreenLantern integrated Ad (by traditional method), the results showed there is no statistical difference in their infectivity (Figure 4G). We also measured each Ad's vDNA amplification at 4, 24, 48, and 72 h post-infection in A549 cells by qPCR and demonstrated there was no difference in their DNA replication kinetics (Figure 4H).

It has been well documented that rescuing *E1*-deleted replication-defective Ads (RD-Ad) in 293-based cell lines can spontaneously generate a rare population of RC-Ads by homologous recombination between RD-Ad genomes and endogenous Ad5 partial gDNA in 293 cells.[37–39] Consistent with the earlier findings, when we used a qPCR primer set that only targets Ad5 *E1* sequences, we observed such a fragment within the total Ad genomes with frequencies about 2×10^{-6} to 2×10^{-5} percent (Figure 4I), indicating that there is recombination events between receiver Ads/integrated Ads and endogenous Ad5 DNA fragments in 293 cells for generating such a population. However, similar contamination levels were observed in both Ads rescued by FastAd or Ads rescued by the traditional method (Figure 4I). To mitigate this risk of Ad5 *E1* recombination, A549-Cre+Bxb1 and A549-FLP cells were generated. Although the rescue efficiency is lower than 293-based cells, which require more rounds of passages to reach decent titers, we also rescued conditionally replicating adenovirus (CRAd) expressing mGreenLantern (Figure S2A), murine OX40L (Figure S2B), and murine CD40L (Figure S2C) in the A549-based cell lines.

Flexible forms of donor DNA and Ad backbones for FastAd

To further simplify the process for generating donor DNA and eliminate steps required for cloning of donor DNA plasmids in bacteria, oligos were designed to contain overhangs with the recombinase recognition sites to form a donor DNA with the structure of *loxP*-GOI-attB-*loxP* (Figure 5A), which can be circularized in Cre-expressing cells. Initially, this approach encountered some technical issues because PCR oligos containing *loxP* sequences can form primer dimers (Figure S3). However, this problem was later solved by amplification of the DNA fragment (*loxP*-mGreenLantern-attB-*loxP*) using iProof DNA polymerase in GC buffer supplemented with 3% DMSO (Figure 5B). When this PCR product was transfected as donor DNA into 293-Cre+Bxb1 cells and co-infected with RC-Ad6-mTagBFP2, at least 45% of cells expressed mGreenLantern (Figure 5C). This result demonstrated that PCR products can serve as FastAd donor DNAs.

We also developed a two-step PCR approach to circumvent the *loxP* primer dimer problem by separately PCR amplifying the GOI with primers containing only one *loxP* sequence at a time (Figure 5D). For example, the influenza A nucleoprotein (NP) cassette (*loxP*-CMV-NP-attB-*loxP*) was amplified by a two-step PCR in a standard PCR master mix (Platinum SuperFi PCR Master Mix) (Figure 5E). To demonstrate that FastAd can be used to engineer other types of Ad vectors, NP was knocked into a pIIIA-deleted single-cycle adenovirus (SC-Ad).[40] To do this, the PCR-amplified CMV-NP cassette was transfected into 293-Cre+Bxb1-pIIIa cells and then infected with a receiver virus (SC-Ad6-empty). After five passages in 293-FLP-pIIIa cells for negative selection and CsCl gradient purification, SC-Ad6-NP was demonstrated to express influenza A NP protein by western blot after infection of A549 cells (Figure 5F).

Rapid production of recombinant Ads by FastAd

After successfully producing high titers of recombinant Ads by FastAd within 18 days after five passages (P5) of negative selection in the 293-FLP cell line (Figure 4A), our next goal was to determine the optimal number of passages of negative selection to find the goldilocks zone between purity, yield, and production time.

Based on earlier results, 5%–14% of GOI integrated viruses and 86%–95% of non-integrated viruses were observed prior to FLP-mediated negative selection (Figure 4D). Although the Ψ of non-integrated Ads can be eliminated upon passage into the FLP-expressing cell line, these Ψ-deleted Ads can still replicate their DNA and compete for resources with the desired GOI-integrated Ad during the initial round of negative selection. This competition may lead to a reduced number of the desired recombinant Ads being packaged and hence result in lower viral titers. To prevent potential loss during a single round of negative selection, we started with a minimum of two rounds of negative selection (P2) in 293-FLP cells and tested this in rescue of an oncolytic CRAd6-mOX40L virus. Integration by Cre+Bxb1 and two rounds of negative selection shortened the time to produce large-scale CsCl-purified virus to 10 days from start to finish (Figure 6A). Under this accelerated protocol, the total yield of CRAd6-mOX40L was 1×10^{12} vp after CsCl gradient purification, which equates to approximately 50–100 oncolytic virus doses for typical studies using mouse models.[41]

multiple comparisons test (****$p \leq 0.0001$). (F) Relative abundance of non-integrated receiver Ad sequences when normalized to hexon copies. Statistics of relative mGreenLantern copies/hexon copies were performed by one-way ANOVA and Tukey's multiple comparisons test (**$p \leq 0.002$, ***$p \leq 0.0002$). (G) Viral particle (vp)/infectious unit (ifu) ratio of receiver Ads, Ads generated by FastAd, or by traditional method (homologous recombination in bacteria). Statistics of genome hexon copies were performed by one-way ANOVA and Tukey's multiple comparisons test (ns, not significant). (H) Viral DNA replication kinetics between receiver Ads, Ads by FastAd, and Ads by the traditional method were analyzed by qPCR. (I) Relative Ad5 *E1* gene recombinant copies by qPCR of receiver Ads, Ads by FastAd and Ads by the traditional method.

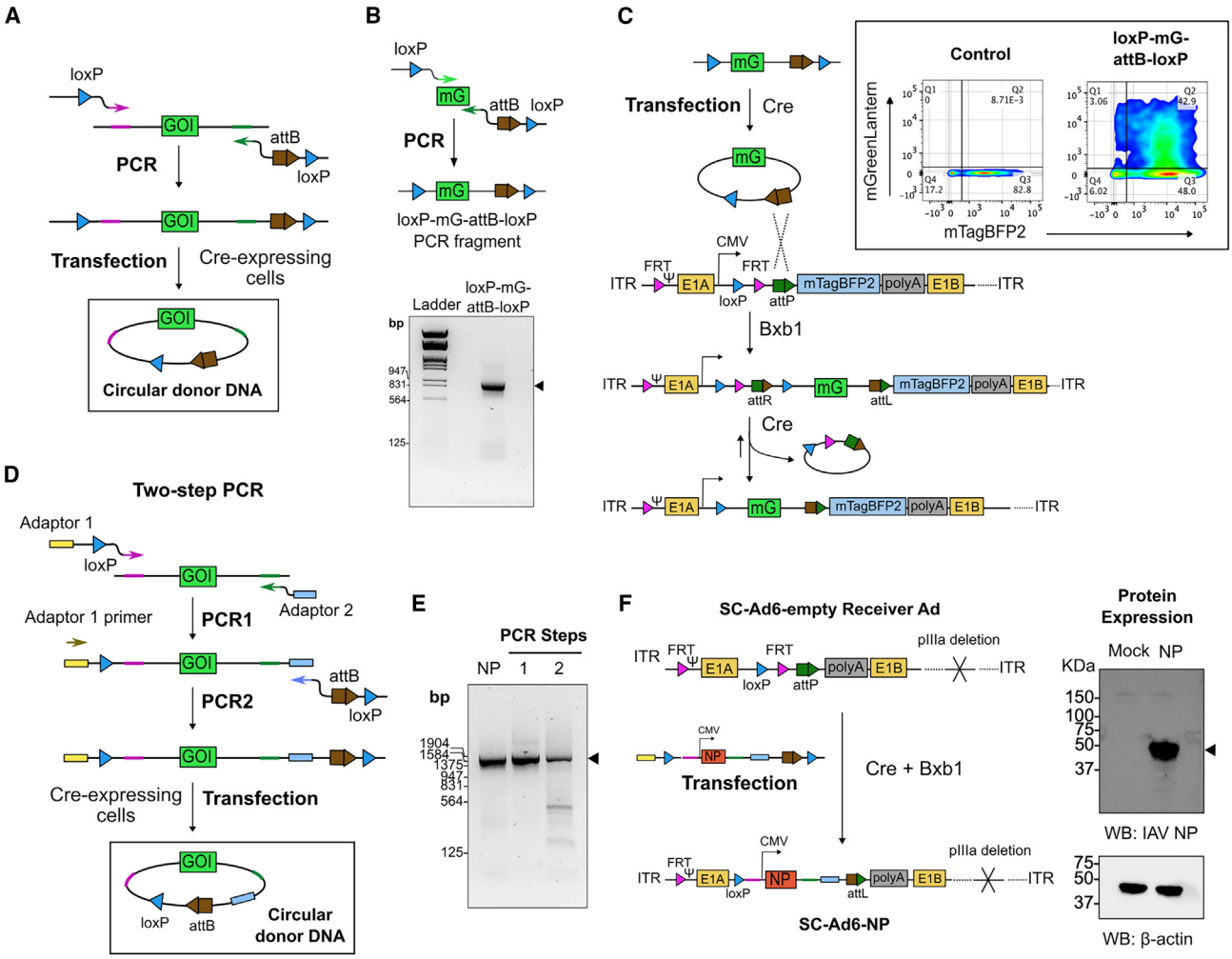

Figure 5. PCR-amplified DNA donors and flexible Ad backbones for FastAd

(A) One-step PCR protocol for the generation of donor DNA fragments containing recombinase recognition sites. (B) Example of one-step PCR amplification of mGreenLantern as DNA donor with the iProof DNA polymerase. (C) Ad backbone diagram and evaluation of the FastAd system using a PCR-amplified mGreenLantern DNA donor. 293-Cre+Bxb1 cells were transfected with or without PCR-amplified *loxP*-mG-attB-*loxP* fragments and infected with RC-Ad-mTagBFP2 for flow cytometry analysis at 48 h post-infection. (D) Two-step PCR protocol for generating the FastAd DNA donors. (E) Representative results of the two-step PCR protocol for the generation of a *loxP*-CMV-NP-attB-*loxP* DNA donor. NP, influenza nucleoprotein cDNA. (F) Ad backbone diagram and western blot analysis of Influenza-NP expression in A549 cells infected with 1,000 vp/cell of FastAd-generated SC-Ad6-NP at 48 h post-infection.

CRAd6-mOX40L produced by this accelerated 10-day rescue protocol was 99.92% pure, with less than 0.08% of the original receiver Ads remaining in the final purified Ad preparation (Figure 6B). Flow cytometry analysis confirmed the expression of mOX40L protein by CRAd6-mOX40L after infection of A549 cells (Figure 6C).

Later, we further passaged this virus for few more rounds into the 293-FLP negative selection cells to compare their purities between different passages. We observed more than 10-fold reduction in receiver Ad copies in the P3 sample when compared with the P2 sample (Figure 6D). However, further negative selection after P3 did not give statistically significant reduction in receiver Ad genome copies. In addition, quantification of Ad5 *E1* gene fragment in purified Ads from each passage demonstrated similar contamination level (1×10^{-6} to 1×10^{-5} percent) of Ad5 *E1* recombinants (Figure 6E).

Overall, these data demonstrate that the FastAd system enables the rapid production of high-titer purified recombinant Ad from donor DNA in just 10 days (P2). However, performing three passages in 293-FLP-negative selection cells (P3) can further reduce receiver Ad contamination, providing an optimal balance between production time, yield, and purity.

Rapid generation of complex adenoviral libraries by FastAd

We next evaluated the ability of FastAd to rapidly generate complex genetic libraries in adenoviral vectors, a task unachievable

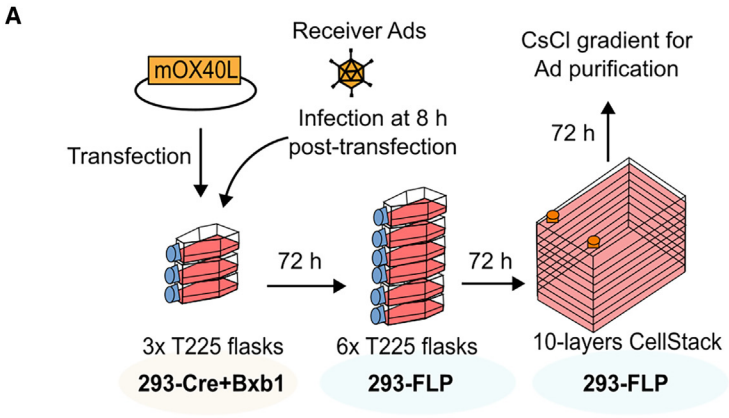

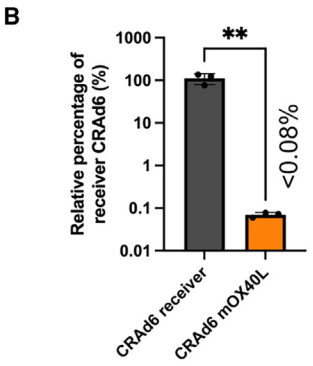

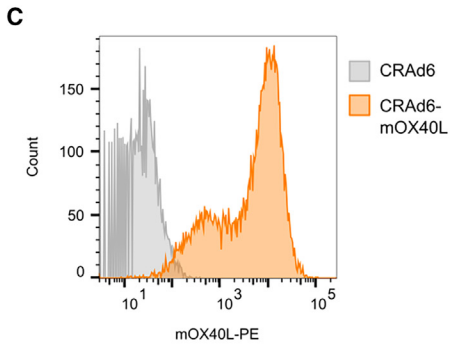

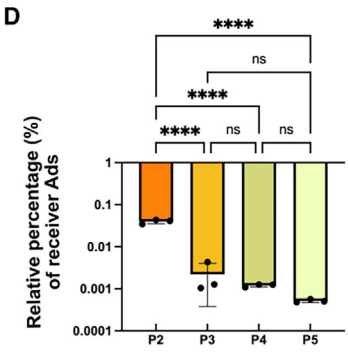

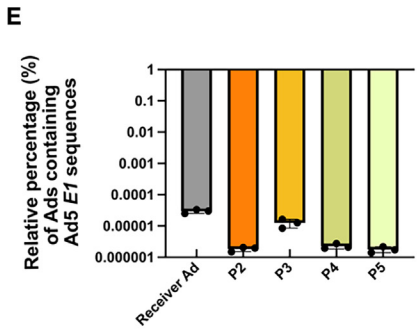

Figure 6. Expedited workflow for producing recombinant Ads with high titers

(A) A 10-day workflow of the FastAd system for amplifying recombinant Ads to the scale of a 10-layer CellSTACK culture chamber. (B) Relative copies of non-integrated receiver CRAd6-CMV normalized to Ad-hexon copies to assess the purity of the Ad generated by the two-round negative selection protocol. (C) Flow cytometry analysis confirmed the expression of mOX40L expression on A549 cells at 48 h post-infection at MOI of 1,000 vp/cell for CRAd6-mOX40L. (D) Relative copies of non-integrated receiver Ads between passages P2, P3, P4, and P5. Statistics were performed by one-way ANOVA and Tukey's multiple comparisons test (****$p \leq 0.0001$). (E) Relative Ad5 *E1* gene recombinant copies by qPCR.

following conventional protocols for Ad cloning and rescue. To quantitatively assess the library size, oligonucleotides containing 17-mer random nucleotides (N17) with up to 1.718×10^{10} variants were synthesized. One-step PCR was used to amplify the N17 sequences and to add FastAd recombinase recognition sites for integration. To confirm the quality and library diversity, this PCR product was first subjected to next-generation sequencing (NGS) to examine library diversity before using it for integration (Figures 7A and 7B). Of the total of 4.35×10^7 output NGS reads, 3.95×10^7 reads mapped to the N17 oligonucleotide, with 3.81×10^7 reads occurring only once (Figure 7C). As expected, the N17 library had a high diversity, with 96.59% of all sequences being unique (Figure 7D), while maintaining an unbiased nucleotide distribution (Figure 7E).

Considering the upper limit of NGS output is about 40 million reads/sample in this study, we started the experiment with a T25 flask scale of transfection to estimate the library diversity. This N17 PCR product library was transfected into a T25 flask of 293-Cre+Bxb1 cells and infected with a receiver virus (RC-Ad6-empty-RSV-mGreenLantern). This population was passaged 5 times in 293-FLP cells from a T25 flask scale (25 cm^2) to reach a 10-layer CellSTACK scale (6,360 cm^2) to be able to be purified on CsCl gradients. The random 17-mer region was subsequently amplified from purified vDNA across three independent replicates and analyzed by NGS (Figures 7F and 7G). The average number of unique reads from the Ad-N17 libraries was 3.01×10^6 from an average of 4.13×10^7 mapped reads (Figure 7H).

While we noted a decrease in library diversity in Ad-N17 libraries compared with the original PCR template (Figures 7D and 7I), it is important to highlight that the library diversity still remains at a million scale. The nucleotide distribution remained unbiased after integration into Ads (Figure 7J). In another pilot study utilizing a 15-mer random library from a different vendor, we observed comparable outcomes (Figure S4).

These results demonstrated that FastAd generated highly diverse genetic libraries with approximately 3 million unique viral clones generated in a T25 flask. This efficiency was in striking contrast with conventional Ad construction methods, which typically yield less than 50 clones per μg of transfected DNA.[17]

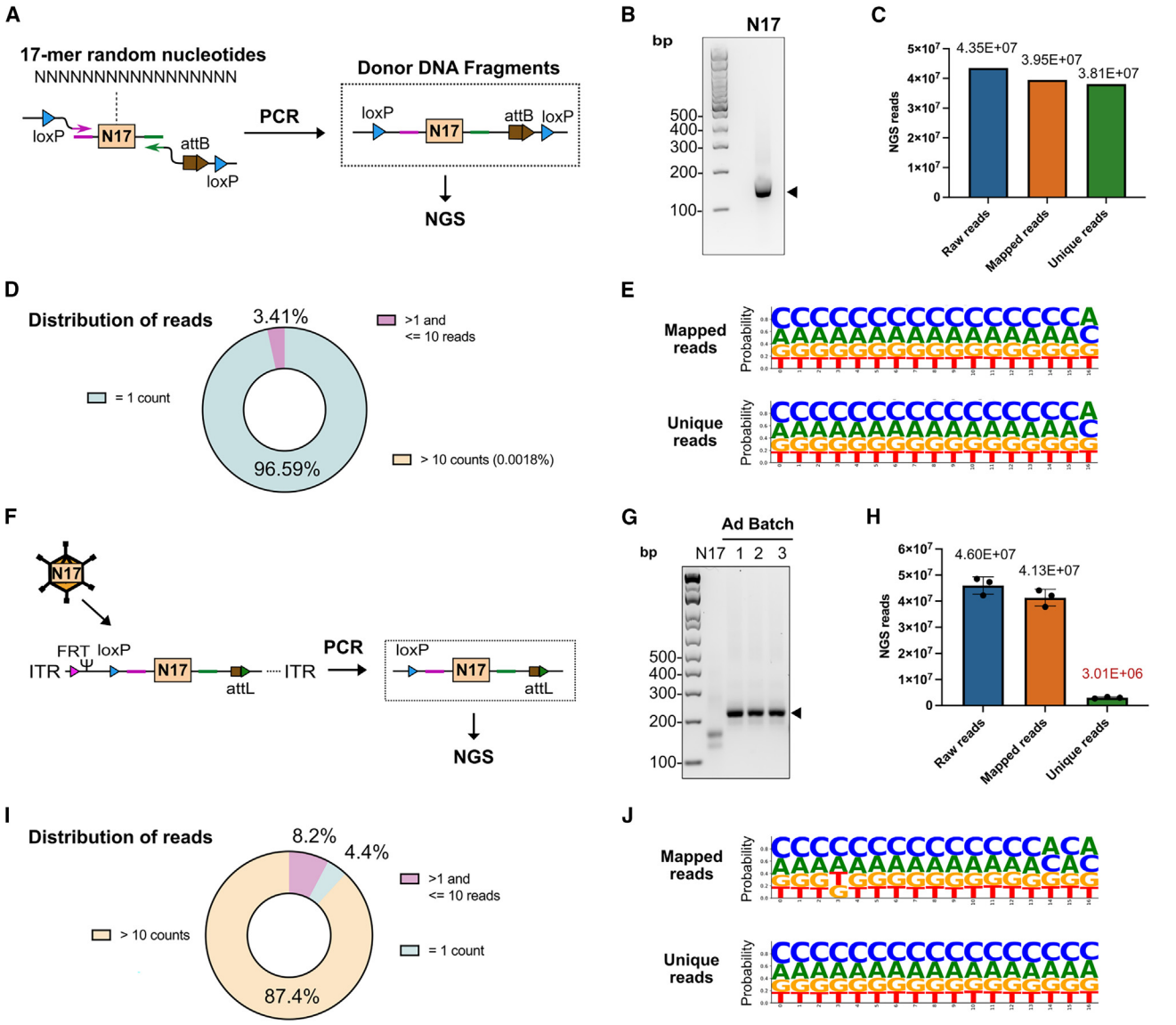

Figure 7. Simple and rapid generation of complex Ad libraries by FastAd

(A) Generating random 17-mer (N17) donor DNA fragments for the FastAd library by one-step PCR amplification of a donor library containing 17-mer random oligonucleotides. (B) Gel electrophoresis to verify PCR amplification of N17 library donor DNA fragments. (C) N17 library donor DNA fragments were analyzed by NGS. Total raw reads, mapped reads, and unique reads are shown. (D) Distribution of reads in categories of unique and multiple occurrences in the N17 library donor DNA fragments. (E) Sequence logo position-based analysis of nucleotide frequency demonstrates an unbiased distribution in the N17 random nucleotides in donor DNA fragments. (F) Extracting N17 library from Ad library. (G) Gel electrophoresis to verify PCR amplification of N17 library donor DNA fragments and N17 libraries from three independent Ad library preparations. (H) N17 libraries from Ad were analyzed by NGS. Total raw reads, mapped reads, and unique reads were shown. (I) Percentage of counts in total mapped sequences from three categories in the N17 Ad library. (J) The sequence logo demonstrating the nucleotide ratio in each position of the N17 random nucleotides in Ad library.

Comprehensive capture of a genome-wide CRISPR-Cas9 gRNA library by FastAd

The GeCKO v2 human genome-wide knockout guide RNA (gRNA) lentiviral library contains 119,418 unique gRNAs.[42] To demonstrate another example using FastAd for constructing an Ad library, we used this gRNA library as a template to generate a FastAd gRNA donor population by two-step PCR (Figures 8A and S5). To speed up the overall production, this donor population was transfected into three T225 flasks of 293-Cre+Bxb1 cells followed by infection with RC-Ad receiver virus (RC-Ad6-empty-RSV-mGreenLantern) and only two passages of viruses in 293-FLP cells (Figure 8B). By this approach, a FastAd gRNA library was generated in only

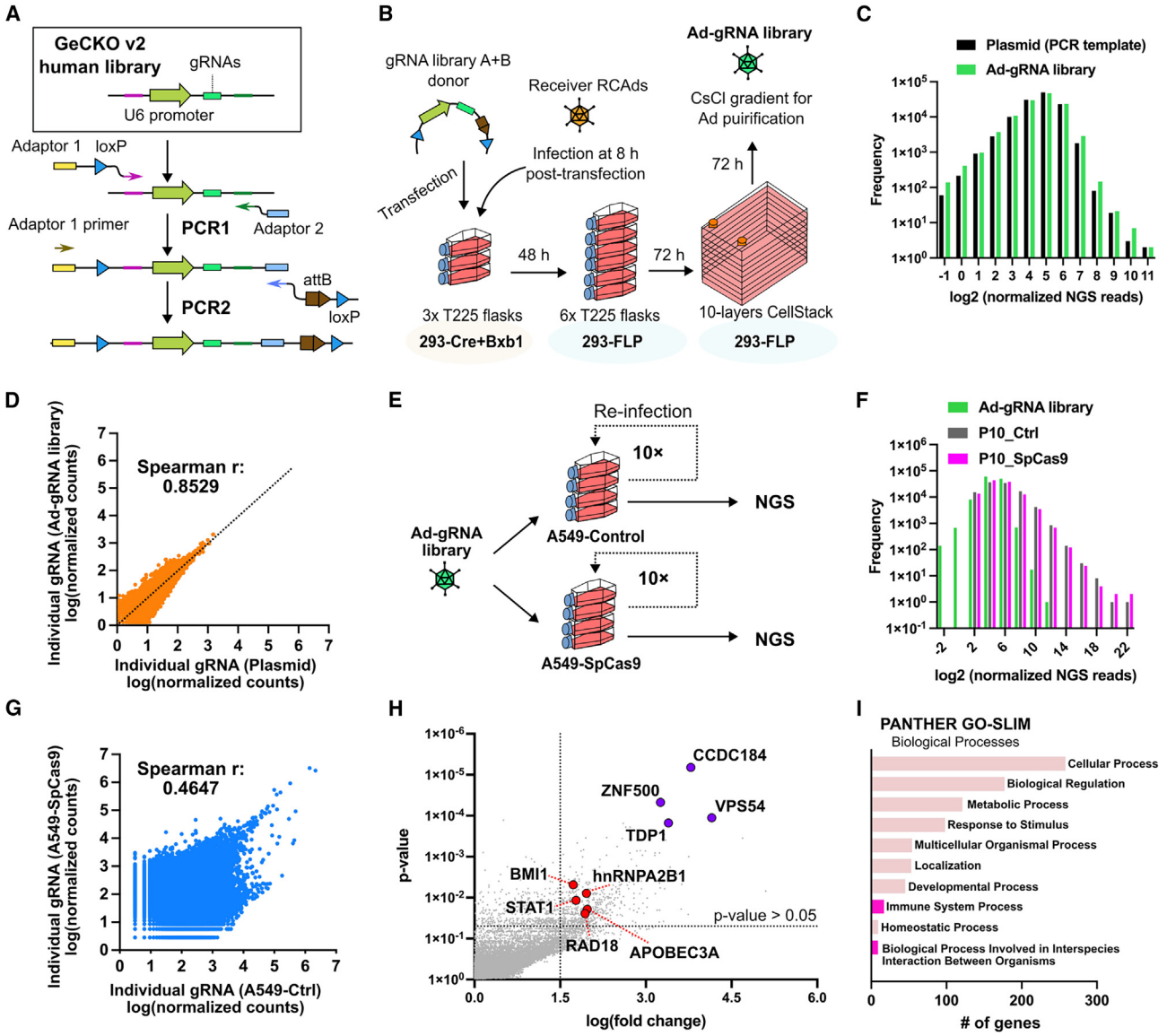

Figure 8. Application of Ad-gRNA library for functional evolution

(A) Schematic for the two-step PCR amplification of the GeCKO v2 human genome-wide knockout gRNA library as FastAd donor DNA. (B) The expedited workflow for transferring the whole gRNA library in Ads by FastAd. (C) gRNA representation in lentiviral plasmid DNA and Ad-gRNA library. Bars represent the number of unique gRNAs with a specific read count. (D) Comparison of gRNA representation in the plasmid library and Ad-gRNA library. (E) Ad-gRNA library was subjected to 10 passages in A549-Ctrl cells or A549-SpCas9 cells followed by NGS analysis of the resulting libraries. (F) Clonal distribution of gRNAs in the input Ad-gRNA library and in Ad-gRNA libraries after 10 passages of evolution. (G) Comparison of gRNA representation between Ad-gRNA selected in A549-Ctrl cells and A549-SpCas9 cells. (H) Identification of enriched target genes in Ad-gRNA library after 10 passages in A549-SpCas9 cells. Genes highlighted in red represent previously reported Ad restriction factors. Genes in purple represent the top 4 enriched genes in the Ad-gRNA library evolution experiment. (I) PANTHER GO-SLIM Gene Ontology (GO) for enriched target genes ($p < 0.05$ and gRNA count fold change >1.5) in Ad-gRNA library after 10 passages in A549-SpCas9 cells.

9 days. NGS analysis of the PCR-amplified gRNAs from the original lentiviral gRNA library and the newly generated Ad-gRNA library demonstrated that the Ad-gRNA library captured 99.97% of the original gRNAs from the GeCKO v2 gRNA lentiviral library (Table S1). Furthermore, the distribution of unique gRNA counts was nearly identical between the original lentiviral library and the Ad-gRNA library (Figure 8C) as demonstrated by a Spearman's rank correlation coefficient of 0.8529 between the gRNA library from lentiviral vectors and the Ad-gRNA library (where r = 1 indicates the highest positive correlation) (Figure 8D). Thus, a complex gRNA library was rapidly transferred into adenoviral vectors by FastAd.

Functional selection of the FastAd gRNA library to identify novel Ad-host interactions

Since the gRNA sequences were encoded by Ads within the Ad-gRNA library, we expect that Ads carrying gRNAs targeting antiviral host genes will likely increase in their clone counts in SpCas9-expressing cells, as the suppressor function of host genes is ablated for better virus propagation.[43] This Ad-gRNA library was passaged in human A549 control (A549-Ctrl) cells, as well as in A549 cells expressing SpCas9, to identify host genes that might inhibit Ad life cycle. Interestingly, gRNAs in the libraries, whether from A549-Ctrl or A549-SpCas9 cells, exhibited right-skewed distributions toward higher clone counts at the 10th passage (P10) (Figure 8F). Although the data show that the distribution of the Ad-gRNA library can drift over time during passaging even without the expression of SpCas9, we indeed observed a low correlation (Spearman's r = 0.4647) between the two libraries (Figure 8G), suggesting that expression of SpCas9 created a selective pressure on the Ad-gRNA population.

Using the sample from A549-Ctrl cells as the control group and the sample from A549-SpCas9 cells as the experimental group in the Model-based Analysis of Genome-wide CRISPR-Cas9 Knockout (MAGeCK) analysis,[44] several host genes were identified to be enriched in the A549-SpCas9 group (Figure 8H; Table S2). Genes previously identified as restriction factors for Ads, including *APOBEC3A*,[45] *BMI1*,[46] *hnRNPA2B1*,[47] *RAD18*,[48] and *STAT1*,[49] were identified, suggesting that the library was properly sampling the genome space. While gRNAs against these previously reported Ad-interacting genes were found to be enriched, the top 4 targeted genes, *CCDC184*, *VPS54*, *ZNF500*, and *TDP1* (with the lowest *p* values and the highest fold changes in gRNA counts), were not previously reported to be associated with Ad restriction (Figure 8H).

The top 565 gene target candidates that enriched in the A549-SpCas9 group were selected based on having a *p* value lower than 0.05 and a gRNA count fold change greater than 1.5 (Table S2). These were subjected to PANTHER GO-slim analysis for Gene Ontology (GO) term enrichment.[50,51] Based on this analysis, enriched terms included immune system process (GO:0002376) and biological processes involved in interspecies interaction between organisms (GO:0044419) (Figure 8I). Nine target gene candidates were identified in the biological processes involved in interspecies interaction between organisms category (GO:0044419) (Table S3), including *IL36G*, *REG3G*, *RFPL4AL1*, *TRIM64B*, and *TRIM64C* host genes, which are not previously described to interact with Ads. This result offers direct insights into unexplored Ad-host interactions for further investigation. Overall, these results demonstrate rapid production and application of an Ad-gRNA library by FastAd to uncover novel virus-host interactions.

DISCUSSION

The bacterial homologous recombination method has long been favored for constructing Ad vectors due to its reliability and ease of use.[13–15] Consequently, most advancements in recombinant Ad technology have been built upon this original protocol.[23] For example, key improvements in adenoviral vector cloning include the use of a single competent cell strain for both DNA recombination and plasmid production,[52] the application of red recombinase to enhance recombination efficiency,[16] the development of stable competent cells preloaded wtih ready-to-recombine adenoviral vectors,[53] the introduction of counter-selection markers for cloning shuttle plasmids or adenoviral backbones,[14,54] and the adoption of modern one-step *in vitro* recombination systems.[55,56] To address the challenges of low virus rescue efficiency from bacteria-derived adenoviral DNA lacking TPs,[21,22] the rescue step was also improved by several methods, such as ligation of TPs to recombinant adenoviral DNA,[57] overexpression of TPs in producer cells,[24] and using the CRISPR-Cas9 system for ITR terminal resolution.[58]

Despite these improvements in both adenoviral vector cloning and rescue steps, the process still requires a minimum of 3 days for vector cloning, followed by an additional 5–7 days for the initial vector rescue in cells,[59] and up to a month of Ad amplification to obtain sufficient yields for *in vivo* animal experiments. Moreover, the low rescue efficiency of adenoviral gDNA lacking TPs limits the output to as few as 50 viral clones per 6×10^8 copies of recombinant adenoviral DNA, thereby restricting the construction of large viral genetic libraries using current methods.[17]

To overcome these challenges, we developed FastAd, a system that integrates transfected DNA fragments into adenoviral genomes in cells via programmed actions of site-specific DNA recombinases. In this study, we prove that FastAd efficiently and rapidly integrates transfected recombinant DNA fragments into designed receiver viruses, induces transgene expression, and can be used to generate complex genetic libraries at an efficiency of approximately one unique viral clone per transfected cell.

Several features make FastAd intrinsically efficient. First, we utilized Bxb1 recombinase and optimized attB/attP sites for the primary integration event of transgenes.[60] Bxb1 induces an irreversible, unidirectional integration of provided donor DNA, leading to an accumulation of integrated Ads over time in the population, while the Cre/*loxP* system primarily mediates DNA fragment shuffling (Figure 3G). Our results demonstrated that FastAd achieves a 100-fold increase in efficiency compared with the Cre/*loxP* system when evaluating the proportion of integrated viruses in the purified virus stock (Figure 4E). Our data also revealed that approximately 5%–14% of Ads were integrated by Cre/Bxb1 (Figure 4D), whereas only 0.1%–0.5% of successful integration events were reported using phage ϕC31 integrase.[61]

Secondly, FastAd's negative selection process ensures that the majority of adenoviral genomes are packaged into virions only when donor DNA is integrated precisely at designated sites within the Ad genome. This mechanism effectively reduces the fraction of receiver Ads in samples and minimizes the risk of off-target integration. Flanking the Ad packaging signal Ψ with FRT or *loxP* sites is a widely adopted mechanism to remove helper viruses for helper-dependent Ad

production.[62] By using the same mechanism, receiver Ad contamination decreases drastically with increasing passages in negative selection cells. Specifically, only two passages in negative selection cell lines already increase the purity of donor-modified Ads to 99.92%, with less than 0.08% of contaminating receiver virus left (Figure 6B).

Preparing donor DNA fragments for FastAd is also significantly simpler than preparing shuttle plasmids in conventional methods, as the modular design of donor DNA allows it to be prepared independently of Ad backbone sequences. Since the DNA fragments for FastAd only needs to be flanked by a 34 bp *loxP* site at the 5′ end and a 74 bp attB site + *loxP* site at the 3′ end, the donor DNA production can be streamlined by incorporating the recombinase recognition sites during gene synthesis or adding them by PCR, enabling a "cloning-free" adenoviral vector construction.

Most importantly, FastAd can achieve a rapid, large-scale Ad production and condenses the current 1- to 2-month production timeline down to 10 days or less. This new workflow not only expedites the Ad production time but also comes with a decent titer and purity of viruses, facilitating, for example, high-throughput screening for testing a variety of genetic payloads (i.e., immune-stimulatory payloads in oncolytic Ads).

However, the final virus stock indeed contains low level contaminations of receiver Ads (Figure 6D), and we believe the contamination levels of receiver Ads are likely to vary from batch to batch. Therefore, users should always carefully evaluate the contamination rates, such as using qPCR, before using the virus stock for any other experiments. We also recommend users to validate results with plaque-purified Ads after the pilot studies with FastAd-generated viruses to avoid any confounding factors that may come from receiver Ads.

As 293 cell lines contains Ad5 left ITR and *E1* gene sequences,[63] we indeed observed low levels of Ad5 *E1* sequences when amplifying our receiver virus stocks and when producing Ads by FastAd in 293-based cell lines (Figure 4I). Despite its low levels, this result suggested that there is a potential risk that the FRT sites next to Ψ and the FastAd cassette inserted between *E1A* and *E1B* genes replaced by homologous recombination in 293 cells, generating rare Ad recombinant populations that can escape counter-selection. To overcome this potential risk in the FastAd system, we have developed A549-based cell lines (Figure S2), which do not contain endogenous wild-type Ad5 genome sequences. However, the 293-based cell lines may still be favored over other cell lines when generating the Ad library due to its high transfection efficiency to introduce complex DNA donors.

Although not demonstrated in this study, FastAd receiver viruses can also be *E1*-delated first-generation RD-Ad vectors. As RD-Ads lack *E1* genes, they are more likely to be outgrown by the RC-Ad contaminants. A better approach to avoid RC-Ad generation is to rescue RD-Ad-based viruses in other *E1*-complementary cell lines with no homology sequence between the helper *E1* genes in-*trans* within cells and the receiver Ad genomes.[64,65] The A549-basd cell lines for FastAd in this study potentially can be used for generating such cell lines.

In addition, FastAd's initial integration step instantly generates a small population of Ads carrying transgene within 3 days in Cre- and Bxb1-expressing cells. These 3-day viruses exist as a mixture of unmodified receiver virus and the desired transgene-integrated vector. Notably, up to 14% of this mixed Ad population carries the desired modification (Figure 4D). In the applications that absolute pure virus stock is required, plaque purification of this 3-day virus mixture on non-293-based FLP-expressing cells can be a faster alternative to traditional methods for isolating a pure virus clone, especially when original virus stock is rescued in 293 cells.

For the construction of complex Ad libraries, we have demonstrated that FastAd can capture over 3 million unique sequences in a T25 flask (Figure 7H) when using 293-based cell lines. To our knowledge, this represents the most complex genetic library generated in Ads and confirmed by NGS to date. The possible reasons for this high capacity can be attributed to the highly efficient DNA fragment integration by Cre/Bxb1 and the presence of intact TPs within viral genomes. Considering that there are roughly 3 million cells in a T25 flask, it implies that, on average, each cell produces one unique viral clone. If one unique clone per cell is indeed the maximum, it is theoretically possible to increase library complexity by scaling up the cell culture. For instance, producing libraries from 1×10^9 cells in a 10-layer CellSTACK could potentially yield libraries with 1×10^9 unique viral clones.

Notably, a previous study also utilized infectious receiver Ads and transfected plasmid DNA for Ad library construction by the Cre/*loxP* system. Their results demonstrated approximately 1×10^4 unique clones from a single well of a 6-well plate.[31] With approximately 1 million cells per well in a 6-well plate, this translates into 0.01 unique viral clone per cell. We speculate that the approximate 100-fold difference in library generation efficiency between the published Cre/*loxP* system and the FastAd system is likely due to the robust unidirectional integration activity of Bxb1 recombinase, as this number is in line with the 100-fold better performance of FastAd compared with the Cre/*loxP* system in our qPCR results (Figures 3G and 4E).

Another group used a similar counter-selection mechanism like FastAd, wherein the left arm of purified TP-containing Ad DNA was used as receiver and the Cre/*loxP* system was used to knock in a high diversity of cDNA libraries.[30] In this effort, an estimated 10^6 clones were generated from 2×10^7 cells, which would equate to 0.05 unique viral clone per cell. However, because this study was conducted before NGS was widely available, their library size estimation is based on the number of plaques from each preparation, rather than documenting unique sequences. Thus, it is challenging to directly compare their library diversity directly with that achieved by FastAd.

For proof-of-concept of library utility, we transferred an existing GeCKO v2 human genome-wide knockout gRNA library from

lentiviral vectors into Ads using FastAd (Figures 8A–8D). We show that this transfer was mediated without obvious biasing to the library sequences. Given that traditional lentivirus-transduced genome-wide knockout pools are often biased toward the identification of key host factors crucial in the early stages of the virus life cycle,[43] this Ad-based gRNA library emerges as a potent tool for uncovering novel viral suppressors acting in later stages of the Ad life cycle, as knockout events occur post virus entry. In this study, alongside several host factors that have been reported to inhibit Ads, we identified yet unreported host factors enriched in our library selection. Among those unreported genes, ZNF500 has been documented to activate the p53-p21-E2F4 signaling axis,[66] suggesting that knocking out the *ZNF500* gene could potentially suppress p53 and enhance cellular proliferation, thereby promoting more robust Ad replication.[67] TDP1 is involved in DNA repair mechanisms in cells.[68] While the role of TDP1 in the Ad life cycle has not yet been specifically reported, DNA repair mechanisms such as the Mre11-Rad50-NBS1 (MRN) complex have been shown to inhibit Ad replication.[69] gRNAs against *VPS54* gene were also enriched. VPS54 is a subunit of the Golgi-associated retrograde protein complex that is involved in intracellular vesicle transport.[70] While a direct relationship to the Ad is unclear, it is possible that VPS54 could impact endosomal trafficking during the Ad life cycle. Finally, gRNAs targeting *CCDC184* gene were also highly enriched in the Ad gRNA library. At present, it is unclear what the function of CCDC184 is and how it might be related to Ad biology. These host genes might be of interest for studying the interplay of Ads and host cell restriction factors.

In this study, the smallest DNA donor we tested is about 60 bp (N17 random nucleotides) into a 35.5 kbp RC-Ad6-empty-RSV-mGreenLantern receiver virus, while the largest DNA donor we tested is about 2 kbp (CMV-NP) for a 32-kbp SC-Ad6-empty receiver virus. Since the integration step of FastAd uses both Cre and Bxb1, the properties of these two recombinases will directly influence the insertion size of DNA fragments. For Bxb1, its insertion efficiency has been reported to be independent of the insert length, with up to 33 kbp insertion length.[71] On the other hand, although the efficiency of Cre is known to be negatively impacted by the increasing distance between the two *loxP* recombination sites,[72] in FastAd, the distance between two *loxP* sites can be restricted by the length of the plasmid backbone region, which is often less than 2 kbp.

In addition, the receiver Ad genome size is critical for determining if the insert size will cause instability in integrated Ads. We expect to generate a viable virus with stable genome if the DNA insertion does not exceed its 105% of full length (~37.8 kbp). However, the efficiency of packaging and viral growth will depend on the final total length of the Ad genome generated.[73,74] In addition, the context of the DNA sequences would significantly affect the virus fitness or cell viability. For example, insertion of a toxic transgene into receiver Ads may reduce the target virus's growth and increase the chance for other opportunistic Ad contaminants to outcompete, such as RC-Ads generated by homologous recombination from 293 cells.

There are alternative designs that can achieve similar outcomes like FastAd. The system could be simplified by using just one recombinase for integration and another recombinase for negative selection. For example, unidirectional *loxP* sites that were reported previously[26] could be used to delete the second negative selection FRT site (counter-selection marker). The Gateway approach might also be mimicked by using incompatible wild-type and GA-mutant attB/attP sites to delete out the FRT site in producer cells utilizing Bxb1 alone. However, either *loxP* mutants or wild-type attB/attP sites of Bxb1 may have lower integration efficiency, so we cannot predict if these changes will improve or reduce the overall efficiency compared with the current FastAd system.

For the integration step of FastAd, there is a chance that the plasmid backbone can be integrated by Cre (Figure S6A), but this intermediate species will be eliminated by FLP in negative selection. However, in rare cases, Bxb1 may integrate the entire plasmid, and subsequent Cre activity may delete the left FRT site, producing an undesired intermediate that can escape negative selection (Figure S6B). Although this population should be minimal, as shuttle plasmids are always transfected first to reduce unprocessed plasmids in cells, negative selection can be further improved by introducing Cre recombinase into FLP-expressing cells to cleave the plasmid backbone flanked by two loxP sites in Ads.

Other improvements could also be applied to the negative selection strategy. Because the efficiency of tyrosine integrases, like Cre or FLP, correlates with the length of DNA sequences between the recognition sites, this constrains the FastAd cassette to be near the Ψ that serves as the checkpoint for FastAd's negative selection. It may be useful to use a large serine recombinase that has no length restriction to execute Ψ excision, although a previous report showed that Ψ flanked by attB/attP sites of phage ϕC31 integrase affects the packaging efficiency of adenoviral DNA.[75] Alternatively, other viral targets such as polyadenylation signals, splice sites, or critical viral proteins may also be harnessed for negative selection.

Recently, several novel serine recombinases have been identified, which might be more efficient than Bxb1.[76] It may be interesting to see if replacing Bxb1 with other newly identified serine recombinases or using an engineered Bxb1[77] can further improve the efficiency of FastAd.

There are also some limitations of FastAd that are worth mentioning. Firstly, the initial receiver Ad must be modified with recombinase target sites, which means it is only applicable for site-specific integration into the Ad backbone, similar to Gateway cloning or Gibson assembly methods of Ads *in vitro*.[55,56] Next, the initial receiver Ad must be rescued by conventional methods into infectious viruses that take about 2 months. However, this one-time investment for making receiver Ads pays off by the ease of generation of variant Ads and the ability to reproduce receiver Ads from stocks. Third, low-level contaminations of receiver Ads or RC-Ads from 293-based cell lines can be present in the resulting

FastAd pool. Even though the contaminating Ads are genetically defined receiver Ads lacking transgenes, it is important to verify the percentage of contamination of Ads in the final pool by qPCR. As discussed previously, A549-based cell lines can be used to avoid recombination events of Ad5 DNA from 293 cells. If absolute purity is required, viruses can be plaque purified in non-293-based FLP-expressing cells after the initial 3-day rescue, followed by the amplification of pure viral clones.

In conclusion, FastAd represents a significant advance in adenoviral vector construction, offering enhanced efficiency, speed, and versatility. It not only shortens virus production timelines to just 10 days or less while maintaining high purity and titer but also facilitates the generation of complex genetic libraries with unique sequences at a million scale for genetic research and screening. Future directions include expanding FastAd's applications for generating cDNA libraries and screening diverse capsid libraries for vector targeting and de-targeting of Ads and other viral vectors. We believe this technology will not only facilitate novel applications of viral vectors but also accelerate research in fundamental virology.

MATERIALS AND METHODS

Construction of donor DNA plasmids and receiver Ads

We utilized the Bxb1 recombinase GA-mutant variant sites for the attB site and the attP site.[60] For proof of concept, a donor plasmid DNA was generated containing the cDNA of green fluorescent protein, *mGreenLantern*[78] and an attB site flanked by two *loxP* sites (pUC57-*loxP*-mGreenLantern-attB-*loxP*) (Table S4). Similar donor plasmids were constructed with other transgenes including *murine TNFSF4* (*mOX40L*) and *murine CD40LG* (*mCD40L*).

A series of receiver Ad plasmid were generated to produce replication-competent Ad (RC-Ad), SC-Ad and CRAds with species C human adenovirus serotype 6 (Ad6) backbone. For example, RC-Ad6-FRT-Ψ-E1A-CMV-*loxP*-FRT-attP-mTagBFP2-bGHpoly(A)-E1B-ΔE3 was derived from the RC-Ad6-ΔE3 Ad vector.[40] An FRT site was introduced on the left side of its packaging signal (Ψ) with an FRT-Zeocin-FRT cassette via red recombination.[16] This plasmid was transformed into FLP-expressing competent cells (DH5/pCP20) to excise the Zeocin selection marker.[16] Next, RC-Ad6-FRT-Ψ-E1A-CMV-*loxP*-FRT-attP-mTagBFP2-bGHpoly(A)-E1B receiver Ad plasmid (RC-Ad6-mTagBFP2) was created by red recombination with a synthetic CMV-*loxP*-FRT-attP-mTagBFP2-bGH poly(A)-ICeuI-Zeo-ICeuI DNA fragment (Table S5). The insertion site of the cassette is between the nucleotides 1,573 and 1,574 bp of Ad6 genome (GenBank: HQ413315.1).[79] This Zeocin cassette was eliminated from the Ad plasmid DNA via ICeuI digestion and self-ligation of the Ad plasmid.

Additional formats of receiver Ad vectors were generated using similar methodologies: RC-Ad6-FRT-Ψ-E1A-*loxP*-FRT-attP-bGHpoly(A)-E1B-ΔE3-RSV-mGreenLantern (RC-Ad6-empty-RSV-mGreenLantern), CRAd6-FRT-Ψ-E1A-d1101/d1107-CMV-*loxP*-FRT-attP-bGHpoly(A)-E1B-ΔE3 (CRAd6-CMV),[41] and SC-Ad6-FRT-Ψ-E1A-*loxP*-FRT-attP-bGHpoly(A)-E1B-ΔIIIa-ΔE3 (SC-Ad6-empty).[40]

Rescue of receiver Ads using plasmid DNA

Ad plasmid DNA was linearized by the restriction enzyme AsiSI (New England Biolabs, Ipswich, MA) at 37°C for 4 h. Linearized DNA (5 μg) was transfected into a T25 flask grown with 293 cells at 95% confluency using Lipofectamine 3000 (Thermo Fisher Scientific, Carlsbad, CA), following the manufacturer's protocol. After an initial viral rescue period of 2 weeks, cell lysates were generated by three freeze-thaw cycles in a dry ice-ethanol bath and the crude viruses were serially passaged in 293 cells for RC-Ad6-based backbones, in A549 cells for the CRAd6-based backbone, or in 293-IIIa cells for SC-Ad6-based backbones.

Purification of recombinant Ads via CsCl gradients

A large scale of receiver viruses was purified from approximately 10^9 cells in 10-layer CellSTACK culture chambers (Corning, Corning, NY). These cell pellets were resuspended in 7 mL of 20 mM HEPES buffer (pH 7.40 and lysed with 2 mL of 5% sodium deoxycholate for 30 min at room temperature, followed by treatment with 150 μL of DNAse I (10 mg/mL) (Sigma-Aldrich, St. Louis, MO), 15 μL of PureLink RNAse A (10 mg/mL) (Thermo Fisher Scientific), and 170 μL of 2 M $MgCl_2$ for an additional 30 min at 37°C. After centrifugation at 3,000 × *g* for 15 min at 4°C, the crude supernatants were subjected to two subsequent CsCl gradients ultracentrifugation runs at 26,000 × *g*. Next, the purified viruses were desalted with PD-10 desalting columns (Cytiva, Marlborough, MA) in sucrose buffer (0.5 M sucrose, 20 mM HEPES). The estimated concentration of vp/mL was determined by measuring the OD_{260} using a NanoDrop Microvolume Spectrophotometer (Thermo Fisher Scientific). ifu was determined using Adeno-X Rapid Titer Kit (Takara Bio, Shiga, Japan) following the manufacturer's protocol.

Plasmids for generating stable cell lines

Plasmids required for stable transfection (pUC57-EF1a-NLS-Cre-IRES-BSD, pUC57-EF1a-HA-Bxb1-IRES-Neo, and pUC57-EF1a-FLP-IRES-BSD) into A549 cells were synthesized by the Custom Gene Synthesis Service (GenScript, Piscataway, NJ).

The plasmids pLV-EF1a-IRES-Puro (Addgene, plasmid no. 85132) and pLV-EF1a-IRES-Blast (Addgene, plasmid no. 85133) were provided by Dr. Tobias Meyer's lab. The plasmid pLV-EF1-FLP-PGK-Neo was a gift from Dr. Javier Alcudia's lab (Addgene, plasmid no. 108544). In addition, the plasmid pCAG-NLS-HA-Bxb1 (Addgene, plasmid no. 51271) was a gift from Dr. Pawel Pelczar's lab, and lentiCas9-Blast (Addgene, plasmid no. 52962) was gifted from Dr. Feng Zhang's lab.

The NLS-HA-Bxb1 fragment was PCR amplified and subsequently inserted into the lentiviral plasmids pLV-EF1a-IRES-Puro and pLV-EF1a-IRES-Blast, resulting in the generation of the pLV-EF1a-NLS-HA-Bxb1-IRES-Puro and pLV-EF1a-NLS-HA-Bxb1-IRES-Blast lentiviral plasmids, respectively. Furthermore, the plasmid

pLV-EF1a-pIIIa-IRES-Puro was created by PCR amplification of the human Ad serotype 6 pIIIa gene, followed by its insertion into the pLV-EF1a-IRES-Puro vector.

Production of lentiviruses

Lentiviruses were generated through co-transfection of 1 μg of pMD.G, 1.5 μg pGGW, and 2.5 μg of the pLV-EF1a lentiviral vector into 293 cells in T25 flasks using Lipofectamine 3000 reagent. After 16 h, the media containing the transfection reagents were replaced with fresh Dulbecco's modified Eagle's medium (DMEM) (Thermo Fisher Scientific) containing 10% (v/v) fetal bovine serum (FBS) and 1× penicillin-streptomycin (Thermo Fisher Scientific). Lentivirus-containing supernatants were harvested at the 48-h time point post-transfection and syringe filtered through a PVDF membrane with a pore size of 0.45 μm.

Cell lines

Human 293 cells were procured from Microbix (Toronto, Ontario, Canada). Human A549 lung carcinoma was obtained from the American Type Culture Collection (ATCC, Manassas, VA).

The 293-Cre (116) cell line, a derivative of the 293 cell line expressing Cre recombinase, was provided by Dr. Philip Ng.[80] The 293-Cre+Bxb1 cell line was generated by lentiviral transduction of 293-Cre cells with LV-EF1a-NLS-HA-Bxb1-IRES-Puro. The 293-Cre+Bxb1-pIIIa cell line was generated by transducing 293-Cre cells sequentially with the LV-EF1a-NLS-HA-Bxb1-IRES-Blast and LV-EF1a-pIIIa-IRES-Puro lentiviruses. The 293-FLP cell line was created by lentiviral transduction of 293 cells with LV-EF1-FLP-PGK-Neo lentivirus. The 293-FLP-pIIIa cell line was derived by transducing the 293-FLP cell line with the pLV-EF1a-pIIIa-IRES-Puro lentivirus.

The A549-Cre+Bxb1 cell line was generated through sequential transfection of linearized pUC57-EF1a-NLS-Cre-IRES-BSD and pUC57-EF1a-HA-Bxb1-IRES-Neo plasmids. The A549-FLP cell line was constructed by transfection of linearized pUC57-EF1a-FLP-IRES-BSD plasmid. A549 control (A549-Ctrl) cells were transduced with the pLV-EF1a-IRES-Blast construct. The A549-SpCas9 cell line was established by lentiviral transduction with lenti-Cas9-Blast.

All stable cell lines were selected using 1 μg/mL of puromycin, 10 μg/mL of blasticidin, or 400 μg/mL of G418, followed by single-cell cloning using the limiting dilution method.

All cell lines were cultured in complete growth medium consisting of DMEM supplemented with 10% (v/v) heat-inactivated FBS and 1× penicillin-streptomycin.

Evaluation of FastAd efficiency and transgene expression using flow cytometry

The efficiency and dynamics of FastAd was assessed with two fluorescent proteins provided from the receiver Ads (RC-Ad6-mTagBFP2) and from the mGreenLantern donor plasmid (pUC57-*loxP*-mGreenLantern-attB-*loxP*). Cells were seeded in a T25 flask at 95% confluency and 5 μg of the mGreenLantern donor plasmid was transfected into the cells using Lipofectamine 3000 as per the manufacturer's instructions. After 16 h, the cells were infected with the receiver virus, RC-Ad6-mTagBFP2, at a MOI of 1,000 vp/cell. Cells were harvested at 48 h post-infection and fixed in 2% (w/v) paraformaldehyde in phosphate-buffered saline (PBS). The fixed cells were analyzed for their mGreenLantern and mTagBFP2 fluorescence by flow cytometry using an LSR II Flow Cytometer (BD Biosciences, Franklin Lakes, NJ). To assess negative selection by FLP, viruses from infected 293-Cre-Bxb1 cells were harvested at 72 h post-infection and subjected to three freeze-thaw cycles. This cleared lysate was used to infect 293-FLP cells and, after 48 h, these cells were analyzed as described.

Real-time qPCR

Total gDNA was extracted from cells using the QIAamp DNA Mini Kit (QIAGEN, Hilden, Germany) according to the manufacturer's instructions. Ad vDNA (vDNA) was isolated using the PureLink Viral RNA/DNA Mini Kit (Thermo Fisher Scientific) from each purified virus stock. SYBR Green PCR Master Mix (Applied Biosystems, Waltham, MA) and TaqMan Universal PCR Master Mix (Applied Biosystems) were used for qPCR experiments with a QuantStudio 3 Real-Time PCR System (Applied Biosystems). Total gDNA (100 ng) or vDNA (4 ng) were used as input template for each 20 μL qPCR reaction. The cycling condition: initial denaturation of templates with 95°C for 10 min, followed by 40 cycles of 95°C denaturation for 15 s and 60°C annealing and extension for 45 s ΔΔCt method was used for relative quantification by using an Ad-hexon gene as the reference gene. To differentiate transfected mGreenLantern donor plasmids and mGreenLantern fragments amplified by viral replication from crude gDNA, DpnI restriction enzyme was used to specifically digest methylated bacterial plasmid DNA while sparing unmethylated, replicated adenoviral DNA. DpnI (60 units) were added to 3 μg of gDNA for 2 h at 37°C. A qPCR primer set (Table S6) targeting the region containing two DpnI sites within the mGreenLantern cDNA was used for qPCR. To discern non-integrated receiver Ads from integrated Ads, qPCR oligonucleotides (Thermo Fisher Scientific) were synthesized to amplify the *loxP*-FRT-attP region (Table S6), which is exclusively present in the original receiver Ads. For characterizing the kinetics of Ad vDNA replication, A549 cells were infected at 1,000 vp/cell for 4, 24, 48, and 72 h with receiver Ad (RC-Ad6-mTagBFP2), Ads made by FastAd, or by the traditional method (bacteria-derived DNA). Infected cells were harvested and total gDNA were purified. gDNA (100 ng) was used as input for each reaction in the SYBR Green qPCR assay targeting the Ad hexon region. The Ad5 *E1* recombinants in purified Ads were detecting by qPCR using a TaqMan probe that targeted Ad5 *E1* gene (Table S6).

Sanger sequencing to evaluate integration efficiency

Sanger sequencing was performed using the CMV primer (Genewiz/Azenta, South Plainfield, NJ) (Table S6), allowing for sequencing of modified regions downstream of the CMV promoter on Ad genomes.

The analysis of the percentage of original receiver Ads and integrated Ads was conducted using BEAT.[36]

Generation of individual transgene DNA donors or pooled library donors by PCR

A 5′-*loxP* overhang and 3′-attB-*loxP* overhangs were generated by a one-step PCR for mGreenLantern, a 15 random-mer (N15) library from custom-oligo synthesis (Thermo Fisher Scientific), and 17 random-mer (N17) library from custom-oligo synthesis (Integrated DNA Technologies IDT, Coralville, IA) using iProof High-Fidelity DNA Polymerase (Bio-Rad, Hercules, CA) in GC buffer supplemented with 3% DMSO. To address primer dimer issues associated with *loxP* on the oligos when using Platinum SuperFi PCR Master Mix (Thermo Fisher Scientific), a two-step PCR method was implemented. The PCR template, RD-Ad5-NP was a gift from Dr. Richard Vile's lab and GecKO v2 human gRNA library (Addgene pooled library no. 1000000049) was a gift from Dr. Feng Zhang's lab.[42] The primer sets are included in Table S6.

Detection of transgene expression by flow cytometry

The expression of mGreenLantern, mOX40L, and mCD40L from CRAd6 was assessed in A549 cells at 48 h post-infection with 1,000 vp/cell. Following infection, cells were harvested and fixed using a 2% paraformaldehyde PBS solution. For surface markers, cells were directly stained with anti-mOX40L-PE (clone: RM134L) and anti-mCD40L-APC (clone: MR1) antibodies (BioLegend, San Diego, CA). The samples were analyzed by BD LSR II Flow Cytometer.

Detection of transgene expression by western blot

A549 cells infected with 1,000 vp/cell of SC-Ad6-NP were harvested at 48 h post-infection. Following this, cells were lysed using RIPA buffer (50 mM Tris-HCl, 150 mM NaCl, 1.0% [v/v] IGEPAL CA-630, 0.5% [w/v] sodium deoxycholate, 1.0 mM EDTA, 0.1% [w/v] SDS [pH 7.4]), and the protein concentration of collected cell lysates were quantified using Pierce BCA Protein Assay Kits (Thermo Fisher Scientific) following the manufacturer's protocol. Western blot analysis was performed using anti-Influenza NP antibody (Invitrogen, no. PA5-32242) (Thermo Fisher Scientific) and anti-β-actin-HRP antibody (sc-47778) (Santa Cruz Biotechnology, Dallas, TX) for probing.

Workflow for producing recombinant Ads using FastAd

For the 18-day production process, 293-Cre+Bxb1 cells in a T25 flask at 95% confluency were transfected with 5 μg of donor DNA plasmids or PCR products. At 16 h post-transfection, cells were infected with 1,000 vp/cell of receiver Ads. After 3 days post-infection, cells were harvested, and freeze-thawed cleared lysates were passaged onto 293-FLP cells. The culture was then amplified through a total of five passages, with each passage incubated for 72 h. This process was repeated to scale-up to a 10-layer CellSTACK culture chamber (6,360 cm^2). For SC-Ad6-based receiver Ads, 293-Cre+Bxb1-pIIIa and 293-FLP-pIIIa were used. For CRAd6-based receiver in A549-based cell lines, the process is identical except for an additional two to three rounds of amplification required in A549-FLP cells.

For the expedited 9- or 10-day production, 293-Cre+Bxb1 cells in three T225 flasks at 95% confluency were transfected with 45 μg of donor DNA plasmids or PCR products per flask. At 8 h post-transfection, cells were subsequently infected with 1,000 vp/cell of receiver CRAd6-CMV or RC-Ad6-empty-RSV-mGreenLantern. Then, after 48–72 h of incubation, 293-Cre+Bxb1 cells were harvested, freeze-thawed three times. After centrifugation, the cleared supernatant was then passaged onto 293-FLP cells for two rounds of negative selection (P2) and amplified to a scale of a 10-layer CellSTACK culture chamber. Purified CRAd6-mOX40L from P2 was passaged in 293-FLP for one (P3), two (P4), and three (P5) more passages to compare the level of receiver Ad contamination.

Evolution of Ad-gRNA library in A549-SpCas9 cells

To select Ads carrying gRNA targeting host restriction factors, four T225 flasks of A549 control cells (A549-Ctrl) or A549-SpCas9 cells were infected with the Ad-gRNA library at a MOI of 50 vp/cell. After 96 h post-infection, cells were harvested and resuspended in 40 mL of 20 mM HEPES buffer (pH 7.4) and subjected to three freeze-thaw cycles. Following centrifugation at 3,000 × *g* for 5 min, 1 mL of supernatant was used to infect the next four T225 flasks. This process was repeated up to passage 9, with subsequent infections of six T225 flasks. At passage 10, a 10-layer CellSTACK culture chamber was infected to allow for CsCl gradient purification.

NGS and data analysis

Incorporated random 15-mer (N15) and 17-mer (N17) sequences, as well as GecKO v2 human gRNA libraries, in the Ad backbones by FastAd were PCR amplified using Platinum SuperFi PCR Master Mix (Thermo Fisher Scientific). The primer sets specifically recognize Ad backbones to ensure the fragments are integrated (Table S6). Library preparation and DNA fragmentation were processed by Genewiz/Azenta. The libraries were sequenced using the Illumina NovaSeq 6000 platform (2 × 150 bp), yielding an estimated 28.5 million paired-end reads per library for the amplicons.

For analyzing NGS data obtained from random nucleotide barcoded N15 and N17 libraries, custom Python scripts were developed for the analysis (Table S7). In addition, for gRNA library selection analysis, we utilized the MAGeCK method[44] (Table S8). GO-term enrichment was conducted by PANTHER.[50,51]

Data visualization and statistics

General graphing and statistical analyses were performed by GraphPad Prism 10 (GraphPad Software, La Jolla, CA). Flow cytometry data were analyzed and visualized using FlowJo version 10.10.0 (BD Biosciences). Sanger sequencing results were visualized by SnapGene software (www.snapgene.com). Sequence Logo for DNA nucleotide distributions within N15 and N17 randomers were generated by Python (Table S7).

DATA AND CODE AVAILABILITY

The raw data for NGS have been deposited in the Sequence Read Archive (SRA) of the National Center for Biotechnology Information (NCBI) with the accession number

(BioProject: PRJNA1102000). Source codes for NGS data analysis has been included in the supplemental data files.

ACKNOWLEDGMENTS

We thank all members in the Department of Molecular Medicine at Mayo Clinic for supportive discussions for this study. This work was supported by funding from Mayo Clinic including the Walter & Lucille Rubin Fund in Infectious Diseases Honoring Michael Camilleri, MD. In addition, Y.-Y.L. conducted this work without external funding, dedicating his personal time and using his own computing resources.

AUTHOR CONTRIBUTIONS

Conceptualization, S.-C.L. and M.A.B.; methodology, S.-C.L. and Y.-Y.L.; software, S.-C.L. and Y.-Y.L.; formal analysis, S.-C.L. and Y.-Y.L.; investigation, S.-C.L. and F.G.M.; writing – original draft, S.-C.L. and M.A.B.; writing – review & editing, Y.-Y.L., F.G.M., and D.A.M.; visualization, S.-C.L. and Y.-Y.L.; supervision, S.-C.L. and M.A.B.; resources, D.A.M. and M.A.B.; funding acquisition, M.A.B.

DECLARATION OF INTERESTS

M.A.B. is the chief scientific officer at Adze Biotechnology. S.C.L. and M.A.B. have filed a patent application on the described technology.

SUPPLEMENTAL INFORMATION

Supplemental information can be found online at https://doi.org/10.1016/j.omtm.2024.101356.

REFERENCES

1. Lu, S.C., and Barry, M.A. (2022). Locked and loaded: engineering and arming oncolytic adenoviruses to enhance anti-tumor immune responses. Expet Opin. Biol. Ther. *22*, 1359–1378. https://doi.org/10.1080/14712598.2022.2139601.

2. Boucher, P., Cui, X., and Curiel, D.T. (2020). Adenoviral vectors for in vivo delivery of CRISPR-Cas gene editors. J. Control. Release *327*, 788–800. https://doi.org/10.1016/j.jconrel.2020.09.003.

3. Cots, D., Bosch, A., and Chillon, M. (2013). Helper dependent adenovirus vectors: progress and future prospects. Curr. Gene Ther. *13*, 370–381. https://doi.org/10.2174/15665232130513121225338.

4. Jacob-Dolan, C., and Barouch, D.H. (2022). COVID-19 Vaccines: Adenoviral Vectors. Annu. Rev. Med. *73*, 41–54. https://doi.org/10.1146/annurev-med-012621-102252.

5. Sakurai, F., Tachibana, M., and Mizuguchi, H. (2022). Adenovirus vector-based vaccine for infectious diseases. Drug Metabol. Pharmacokinet. *42*, 100432. https://doi.org/10.1016/j.dmpk.2021.100432.

6. Joe, C.C.D., Chopra, N., Nestola, P., Niemann, J., and Douglas, A.D. (2023). Rapid-response manufacturing of adenovirus-vectored vaccines. Nat. Biotechnol. *41*, 314–316. https://doi.org/10.1038/s41587-023-01682-2.

7. Stow, N.D. (1981). Cloning of a DNA fragment from the left-hand terminus of the adenovirus type 2 genome and its use in site-directed mutagenesis. J. Virol. *37*, 171–180. https://doi.org/10.1128/JVI.37.1.171-180.1981.

8. Mizuguchi, H., and Kay, M.A. (1998). Efficient construction of a recombinant adenovirus vector by an improved in vitro ligation method. Hum. Gene Ther. *9*, 2577–2583. https://doi.org/10.1089/hum.1998.9.17-2577.

9. McGrory, W.J., Bautista, D.S., and Graham, F.L. (1988). A simple technique for the rescue of early region I mutations into infectious human adenovirus type 5. Virology *163*, 614–617. https://doi.org/10.1016/0042-6822(88)90302-9.

10. Parks, R., Cummings, D., Evelegh, C., Sankar, U., Graham, F., and Graham, F.L. (1999). A high-efficiency Cre/loxP-based system for construction of adenoviral vectors. Hum. Gene Ther. *10*, 2667–2672. https://doi.org/10.1089/10430349950016708.

11. Bett, A.J., Haddara, W., Prevec, L., and Graham, F.L. (1994). An efficient and flexible system for construction of adenovirus vectors with insertions or deletions in early regions 1 and 3. Proc. Natl. Acad. Sci. USA *91*, 8802–8806. https://doi.org/10.1073/pnas.91.19.8802.

12. Ng, P., Cummings, D.T., Evelegh, C.M., and Graham, F.L. (2000). Yeast recombinase FLP functions effectively in human cells for construction of adenovirus vectors. Biotechniques *29*, 524–528. https://doi.org/10.2144/00293st04.

13. Chartier, C., Degryse, E., Gantzer, M., Dieterle, A., Pavirani, A., and Mehtali, M. (1996). Efficient generation of recombinant adenovirus vectors by homologous recombination in Escherichia coli. J. Virol. *70*, 4805–4810. https://doi.org/10.1128/JVI.70.7.4805-4810.1996.

14. Crouzet, J., Naudin, L., Orsini, C., Vigne, E., Ferrero, L., Le Roux, A., Benoit, P., Latta, M., Torrent, C., Branellec, D., et al. (1997). Recombinational construction in Escherichia coli of infectious adenoviral genomes. Proc. Natl. Acad. Sci. USA *94*, 1414–1419. https://doi.org/10.1073/pnas.94.4.1414.

15. He, T.C., Zhou, S., da Costa, L.T., Yu, J., Kinzler, K.W., and Vogelstein, B. (1998). A simplified system for generating recombinant adenoviruses. Proc. Natl. Acad. Sci. USA *95*, 2509–2514. https://doi.org/10.1073/pnas.95.5.2509.

16. Campos, S.K., and Barry, M.A. (2004). Rapid construction of capsid-modified adenoviral vectors through bacteriophage lambda Red recombination. Hum. Gene Ther. *15*, 1125–1130. https://doi.org/10.1089/hum.2004.15.1125.

17. Elahi, S.M., Oualikene, W., Naghdi, L., O'Connor-McCourt, M., and Massie, B. (2002). Adenovirus-based libraries: efficient generation of recombinant adenoviruses by positive selection with the adenovirus protease. Gene Ther. *9*, 1238–1246. https://doi.org/10.1038/sj.gt.3301793.

18. Schaack, J., Ho, W.Y., Freimuth, P., and Shenk, T. (1990). Adenovirus terminal protein mediates both nuclear matrix association and efficient transcription of adenovirus DNA. Genes Dev. *4*, 1197–1208. https://doi.org/10.1101/gad.4.7.1197.

19. Webster, A., Leith, I.R., Nicholson, J., Hounsell, J., and Hay, R.T. (1997). Role of preterminal protein processing in adenovirus replication. J. Virol. *71*, 6381–6389. https://doi.org/10.1128/JVI.71.9.6381-6389.1997.

20. Al-Wassiti, H.A., Thomas, D.R., Wagstaff, K.M., Fabb, S.A., Jans, D.A., Johnston, A.P., and Pouton, C.W. (2021). Adenovirus Terminal Protein Contains a Bipartite Nuclear Localisation Signal Essential for Its Import into the Nucleus. Int. J. Mol. Sci. *22*, 3310. https://doi.org/10.3390/ijms22073310.

21. Jones, N., and Shenk, T. (1978). Isolation of deletion and substitution mutants of adenovirus type 5. Cell *13*, 181–188. https://doi.org/10.1016/0092-8674(78)90148-4.

22. Miyake, S., Makimura, M., Kanegae, Y., Harada, S., Sato, Y., Takamori, K., Tokuda, C., and Saito, I. (1996). Efficient generation of recombinant adenoviruses using adenovirus DNA-terminal protein complex and a cosmid bearing the full-length virus genome. Proc. Natl. Acad. Sci. USA *93*, 1320–1324. https://doi.org/10.1073/pnas.93.3.1320.

23. Luo, J., Deng, Z.L., Luo, X., Tang, N., Song, W.X., Chen, J., Sharff, K.A., Luu, H.H., Haydon, R.C., Kinzler, K.W., et al. (2007). A protocol for rapid generation of recombinant adenoviruses using the AdEasy system. Nat. Protoc. *2*, 1236–1247. https://doi.org/10.1038/nprot.2007.135.

24. Wu, N., Zhang, H., Deng, F., Li, R., Zhang, W., Chen, X., Wen, S., Wang, N., Zhang, J., Yin, L., et al. (2014). Overexpression of Ad5 precursor terminal protein accelerates recombinant adenovirus packaging and amplification in HEK-293 packaging cells. Gene Ther. *21*, 629–637. https://doi.org/10.1038/gt.2014.40.

25. Planas, D., Staropoli, I., Michel, V., Lemoine, F., Donati, F., Prot, M., Porrot, F., Guivel-Benhassine, F., Jeyarajah, B., Brisebarre, A., et al. (2024). Distinct evolution of SARS-CoV-2 Omicron XBB and BA.2.86/JN.1 lineages combining increased fitness and antibody evasion. Nat. Commun. *15*, 2254. https://doi.org/10.1038/s41467-024-46490-7.

26. Lupold, S.E., Kudrolli, T.A., Chowdhury, W.H., Wu, P., and Rodriguez, R. (2007). A novel method for generating and screening peptides and libraries displayed on adenovirus fiber. Nucleic Acids Res. *35*, e138. https://doi.org/10.1093/nar/gkm914.

27. Miura, Y., Yamasaki, S., Davydova, J., Brown, E., Aoki, K., Vickers, S., and Yamamoto, M. (2013). Infectivity-selective oncolytic adenovirus developed by high-throughput screening of adenovirus-formatted library. Mol. Ther. *21*, 139–148. https://doi.org/10.1038/mt.2012.205.

28. Hatanaka, K., Ohnami, S., Yoshida, K., Miura, Y., Aoyagi, K., Sasaki, H., Asaka, M., Terada, M., Yoshida, T., and Aoki, K. (2003). A simple and efficient method for constructing an adenoviral cDNA expression library. Mol. Ther. *8*, 158–166. https://doi.org/10.1016/s1525-0016(03)00138-2.

29. Hardy, S., Kitamura, M., Harris-Stansil, T., Dai, Y., and Phipps, M.L. (1997). Construction of adenovirus vectors through Cre-lox recombination. J. Virol. *71*, 1842–1849. https://doi.org/10.1128/JVI.71.3.1842-1849.1997.

30. Hillgenberg, M., Hofmann, C., Stadler, H., and Loser, P. (2006). High-efficiency system for the construction of adenovirus vectors and its application to the generation of representative adenovirus-based cDNA expression libraries. J. Virol. *80*, 5435–5450. https://doi.org/10.1128/JVI.00218-06.

31. Yamamoto, Y., Goto, N., Miura, K., Narumi, K., Ohnami, S., Uchida, H., Miura, Y., Yamamoto, M., and Aoki, K. (2014). Development of a novel efficient method to construct an adenovirus library displaying random peptides on the fiber knob. Mol. Pharm. *11*, 1069–1074. https://doi.org/10.1021/mp4005854.

32. Ghosh, P., Kim, A.I., and Hatfull, G.F. (2003). The orientation of mycobacteriophage Bxb1 integration is solely dependent on the central dinucleotide of attP and attB. Mol. Cell *12*, 1101–1111. https://doi.org/10.1016/s1097-2765(03)00444-1.

33. Merrick, C.A., Zhao, J., and Rosser, S.J. (2018). Serine Integrases: Advancing Synthetic Biology. ACS Synth. Biol. *7*, 299–310. https://doi.org/10.1021/acssynbio.7b00308.

34. Ng, P., Beauchamp, C., Evelegh, C., Parks, R., and Graham, F.L. (2001). Development of a FLP/frt system for generating helper-dependent adenoviral vectors. Mol. Ther. *3*, 809–815. https://doi.org/10.1006/mthe.2001.0323.

35. Wilson, V.G. (2012). Cell culture assay for transient replication of human and animal papillomaviruses. Curr Protoc Microbiol *14*, Unit14B.11. https://doi.org/10.1002/9780471729259.mc14b01s24.

36. Xu, L., Liu, Y., and Han, R. (2019). BEAT: A Python Program to Quantify Base Editing from Sanger Sequencing. CRISPR J. *2*, 223–229. https://doi.org/10.1089/crispr.2019.0017.

37. Lochmuller, H., Jani, A., Huard, J., Prescott, S., Simoneau, M., Massie, B., Karpati, G., and Acsadi, G. (1994). Emergence of early region 1-containing replication-competent adenovirus in stocks of replication-defective adenovirus recombinants (delta E1 + delta E3) during multiple passages in 293 cells. Hum. Gene Ther. *5*, 1485–1491. https://doi.org/10.1089/hum.1994.5.12-1485.

38. Hehir, K.M., Armentano, D., Cardoza, L.M., Choquette, T.L., Berthelette, P.B., White, G.A., Couture, L.A., Everton, M.B., Keegan, J., Martin, J.M., et al. (1996). Molecular characterization of replication-competent variants of adenovirus vectors and genome modifications to prevent their occurrence. J. Virol. *70*, 8459–8467. https://doi.org/10.1128/JVI.70.12.8459-8467.1996.

39. Lin, Y.C., Boone, M., Meuris, L., Lemmens, I., Van Roy, N., Soete, A., Reumers, J., Moisse, M., Plaisance, S., Drmanac, R., et al. (2014). Genome dynamics of the human embryonic kidney 293 lineage in response to cell biology manipulations. Nat. Commun. *5*, 4767. https://doi.org/10.1038/ncomms5767.

40. Crosby, C.M., and Barry, M.A. (2014). IIIa deleted adenovirus as a single-cycle genome replicating vector. Virology *462–463*, 158–165. https://doi.org/10.1016/j.virol.2014.05.030.

41. Doronin, K., Toth, K., Kuppuswamy, M., Ward, P., Tollefson, A.E., and Wold, W.S.M. (2000). Tumor-specific, replication-competent adenovirus vectors overexpressing the adenovirus death protein. J. Virol. *74*, 6147–6155. https://doi.org/10.1128/jvi.74.13.6147-6155.2000.

42. Sanjana, N.E., Shalem, O., and Zhang, F. (2014). Improved vectors and genome-wide libraries for CRISPR screening. Nat. Methods *11*, 783–784. https://doi.org/10.1038/nmeth.3047.

43. King, C.R., Liu, Y., Amato, K.A., Schaack, G.A., Mickelson, C., Sanders, A.E., Hu, T., Gupta, S., Langlois, R.A., Smith, J.A., and Mehle, A. (2023). Pathogen-driven CRISPR screens identify TREX1 as a regulator of DNA self-sensing during influenza virus infection. Cell Host Microbe *31*, 1552–1567.e8. https://doi.org/10.1016/j.chom.2023.08.001.

44. Li, W., Xu, H., Xiao, T., Cong, L., Love, M.I., Zhang, F., Irizarry, R.A., Liu, J.S., Brown, M., and Liu, X.S. (2014). MAGeCK enables robust identification of essential genes from genome-scale CRISPR/Cas9 knockout screens. Genome Biol. *15*, 554. https://doi.org/10.1186/s13059-014-0554-4.

45. Gottig, L., Weiss, C., Stubbe, M., Hanrieder, L., Hofmann, S., Grodziecki, A., Stadler, D., Carpentier, A., Protzer, U., and Schreiner, S. (2023). Apobec3A Deamination Functions Are Involved in Antagonizing Efficient Human Adenovirus Replication and Gene Expression. mBio *14*, e0347822. https://doi.org/10.1128/mbio.03478-22.

46. Na, M., Chen, D., Holmqvist, B., Ran, L., Jin, J., Rebetz, J., and Fan, X. (2014). Adenovirus assembly is impaired by BMI1-related histone deacetylase activity. Virology *456–457*, 227–237. https://doi.org/10.1016/j.virol.2014.03.025.

47. Wang, L., Wen, M., and Cao, X. (2019). Nuclear hnRNPA2B1 initiates and amplifies the innate immune response to DNA viruses. Science *365*, eaav0758. https://doi.org/10.1126/science.aav0758.

48. Lloyd, A.G., Tateishi, S., Bieniasz, P.D., Muesing, M.A., Yamaizumi, M., and Mulder, L.C.F. (2006). Effect of DNA repair protein Rad18 on viral infection. PLoS Pathog. *2*, e40. https://doi.org/10.1371/journal.ppat.0020040.

49. Sohn, S.Y., and Hearing, P. (2011). Adenovirus sequesters phosphorylated STAT1 at viral replication centers and inhibits STAT dephosphorylation. J. Virol. *85*, 7555–7562. https://doi.org/10.1128/JVI.00513-11.

50. Mi, H., Muruganujan, A., Ebert, D., Huang, X., and Thomas, P.D. (2019). PANTHER version 14: more genomes, a new PANTHER GO-slim and improvements in enrichment analysis tools. Nucleic Acids Res. *47*, D419–D426. https://doi.org/10.1093/nar/gky1038.

51. Thomas, P.D., Ebert, D., Muruganujan, A., Mushayahama, T., Albou, L.P., and Mi, H. (2022). PANTHER: Making genome-scale phylogenetics accessible to all. Protein Sci. *31*, 8–22. https://doi.org/10.1002/pro.4218.

52. Renaut, L., Bernard, C., and D'Halluin, J.C. (2002). A rapid and easy method for production and selection of recombinant adenovirus genomes. J. Virol. Methods *100*, 121–131. https://doi.org/10.1016/s0166-0934(01)00407-4.

53. Zeng, M., Smith, S.K., Siegel, F., Shi, Z., Kampen, K.V., Elmets, C.A., and Tang, D.C. (2001). AdEasy system made easier by selecting the viral backbone plasmid preceding homologous recombination. Biotechniques *31*, 260–262. https://doi.org/10.2144/01312bm04.

54. Wu, C., Nerurkar, V.R., Yanagihara, R., and Lu, Y. (2008). Effective modifications for improved homologous recombination and high-efficiency generation of recombinant adenovirus-based vectors. J. Virol. Methods *153*, 120–128. https://doi.org/10.1016/j.jviromet.2008.07.024.

55. Yang, Y., Chi, Y., Tang, X., Ertl, H.C., and Zhou, D. (2016). Rapid, Efficient, and Modular Generation of Adenoviral Vectors via Isothermal Assembly. Curr. Protoc. Mol. Biol. *113*, 16.26.1–16.26.18. https://doi.org/10.1002/0471142727.mb1626s113.

56. Choi, E.W., Seen, D.S., Song, Y.B., Son, H.S., Jung, N.C., Huh, W.K., Hahn, J.S., Kim, K., Jeong, J.Y., and Lee, T.G. (2012). AdHTS: a high-throughput system for generating recombinant adenoviruses. J. Biotechnol. *162*, 246–252. https://doi.org/10.1016/j.jbiotec.2012.10.001.

57. Okada, T., Ramsey, W.J., Munir, J., Wildner, O., and Blaese, R.M. (1998). Efficient directional cloning of recombinant adenovirus vectors using DNA-protein complex. Nucleic Acids Res. *26*, 1947–1950. https://doi.org/10.1093/nar/26.8.1947.

58. Riedl, A., Fischer, J., Burgert, H.G., and Ruzsics, Z. (2022). Rescue of Recombinant Adenoviruses by CRISPR/Cas-Mediated in vivo Terminal Resolution. Front. Microbiol. *13*, 854690. https://doi.org/10.3389/fmicb.2022.854690.

59. Ni, N., Deng, F., He, F., Wang, H., Shi, D., Liao, J., Zou, Y., Wang, H., Zhao, P., Hu, X., et al. (2021). A one-step construction of adenovirus (OSCA) system using the Gibson DNA Assembly technology. Mol Ther Oncolytics *23*, 602–611. https://doi.org/10.1016/j.omto.2021.11.011.

60. Jusiak, B., Jagtap, K., Gaidukov, L., Duportet, X., Bandara, K., Chu, J., Zhang, L., Weiss, R., and Lu, T.K. (2019). Comparison of Integrases Identifies Bxb1-GA Mutant as the Most Efficient Site-Specific Integrase System in Mammalian Cells. ACS Synth. Biol. *8*, 16–24. https://doi.org/10.1021/acssynbio.8b00089.

61. Robert, M.A., Zeng, Y., Raymond, B., Desfossé, L., Mairey, E., Tremblay, J.P., Massie, B., and Gilbert, R. (2012). Efficacy and site-specificity of adenoviral vector integration mediated by the phage ϕC31 integrase. Hum. Gene Ther. Methods *23*, 393–407. https://doi.org/10.1089/hgtb.2012.122.

62. Rosewell, A., Vetrini, F., and Ng, P. (2011). Helper-Dependent Adenoviral Vectors. J Genet Syndr Gene. *5*, 001. https://doi.org/10.4172/2157-7412.s5-001.

63. Louis, N., Evelegh, C., and Graham, F.L. (1997). Cloning and sequencing of the cellular-viral junctions from the human adenovirus type 5 transformed 293 cell line. Virology *233*, 423–429. https://doi.org/10.1006/viro.1997.8597.

64. Farson, D., Tao, L., Ko, D., Li, Q., Brignetti, D., Segawa, K., Mittelstaedt, D., Harding, T., Yu, D.C., and Li, Y. (2006). Development of novel E1-complementary cells for

adenoviral production free of replication-competent adenovirus. Mol. Ther. *14*, 305–311. https://doi.org/10.1016/j.ymthe.2006.02.020.

65. Fallaux, F.J., Bout, A., van der Velde, I., van den Wollenberg, D.J.M., Hehir, K.M., Keegan, J., Auger, C., Cramer, S.J., van Ormondt, H., van der Eb, A.J., et al. (1998). New helper cells and matched early region 1-deleted adenovirus vectors prevent generation of replication-competent adenoviruses. Hum. Gene Ther. *9*, 1909–1917. https://doi.org/10.1089/hum.1998.9.13-1909.

66. Ma, X., Fan, M., Yang, K., Wang, Y., Hu, R., Guan, M., Hou, Y., Ying, J., Deng, N., Li, Q., et al. (2023). ZNF500 abolishes breast cancer proliferation and sensitizes chemotherapy by stabilizing P53 via competing with MDM2. Cancer Sci. *114*, 4237–4251. https://doi.org/10.1111/cas.15947.

67. Li, Q., Zhao, L.Y., Zheng, Z., Yang, H., Santiago, A., and Liao, D. (2011). Inhibition of p53 by adenovirus type 12 E1B-55K deregulates cell cycle control and sensitizes tumor cells to genotoxic agents. J. Virol. *85*, 7976–7988. https://doi.org/10.1128/JVI.00492-11.

68. Pommier, Y., Huang, S.y.N., Gao, R., Das, B.B., Murai, J., and Marchand, C. (2014). Tyrosyl-DNA-phosphodiesterases (TDP1 and TDP2). DNA Repair *19*, 114–129. https://doi.org/10.1016/j.dnarep.2014.03.020.

69. Weitzman, M.D., and Ornelles, D.A. (2005). Inactivating intracellular antiviral responses during adenovirus infection. Oncogene *24*, 7686–7696. https://doi.org/10.1038/sj.onc.1209063.

70. Wei, J., Zhang, Y.Y., Luo, J., Wang, J.Q., Zhou, Y.X., Miao, H.H., Shi, X.J., Qu, Y.X., Xu, J., Li, B.L., and Song, B.L. (2017). The GARP Complex Is Involved in Intracellular Cholesterol Transport via Targeting NPC2 to Lysosomes. Cell Rep. *19*, 2823–2835. https://doi.org/10.1016/j.celrep.2017.06.012.

71. Gaidukov, L., Wroblewska, L., Teague, B., Nelson, T., Zhang, X., Liu, Y., Jagtap, K., Mamo, S., Tseng, W.A., Lowe, A., et al. (2018). A multi-landing pad DNA integration platform for mammalian cell engineering. Nucleic Acids Res. *46*, 4072–4086. https://doi.org/10.1093/nar/gky216.

72. Zheng, B., Sage, M., Sheppeard, E.A., Jurecic, V., and Bradley, A. (2000). Engineering mouse chromosomes with Cre-loxP: range, efficiency, and somatic applications. Mol. Cell Biol. *20*, 648–655. https://doi.org/10.1128/MCB.20.2.648-655.2000.

73. Bett, A.J., Prevec, L., and Graham, F.L. (1993). Packaging capacity and stability of human adenovirus type 5 vectors. J. Virol. *67*, 5911–5921. https://doi.org/10.1128/JVI.67.10.5911-5921.1993.

74. Parks, R.J., and Graham, F.L. (1997). A helper-dependent system for adenovirus vector production helps define a lower limit for efficient DNA packaging. J. Virol. *71*, 3293–3298. https://doi.org/10.1128/JVI.71.4.3293-3298.1997.

75. Alba, R., Hearing, P., Bosch, A., and Chillon, M. (2007). Differential amplification of adenovirus vectors by flanking the packaging signal with attB/attP-PhiC31 sequences: implications for helper-dependent adenovirus production. Virology *367*, 51–58. https://doi.org/10.1016/j.virol.2007.05.014.

76. Durrant, M.G., Fanton, A., Tycko, J., Hinks, M., Chandrasekaran, S.S., Perry, N.T., Schaepe, J., Du, P.P., Lotfy, P., Bassik, M.C., et al. (2023). Systematic discovery of recombinases for efficient integration of large DNA sequences into the human genome. Nat. Biotechnol. *41*, 488–499. https://doi.org/10.1038/s41587-022-01494-w.

77. Pandey, S., Gao, X.D., Krasnow, N.A., McElroy, A., Tao, Y.A., Duby, J.E., Steinbeck, B.J., McCreary, J., Pierce, S.E., Tolar, J., et al. (2024). Efficient site-specific integration of large genes in mammalian cells via continuously evolved recombinases and prime editing. Nat. Biomed. Eng. https://doi.org/10.1038/s41551-024-01227-1.

78. Campbell, B.C., Nabel, E.M., Murdock, M.H., Lao-Peregrin, C., Tsoulfas, P., Blackmore, M.G., Lee, F.S., Liston, C., Morishita, H., and Petsko, G.A. (2020). mGreenLantern: a bright monomeric fluorescent protein with rapid expression and cell filling properties for neuronal imaging. Proc. Natl. Acad. Sci. USA *117*, 30710–30721. https://doi.org/10.1073/pnas.2000942117.

79. Shashkova, E.V., Doronin, K., Senac, J.S., and Barry, M.A. (2008). Macrophage depletion combined with anticoagulant therapy increases therapeutic window of systemic treatment with oncolytic adenovirus. Cancer Res. *68*, 5896–5904. https://doi.org/10.1158/0008-5472.CAN-08-0488.

80. Palmer, D., and Ng, P. (2003). Improved system for helper-dependent adenoviral vector production. Mol. Ther. *8*, 846–852. https://doi.org/10.1016/j.ymthe.2003.08.014.